NGR-47-004-129

COLLEGE OF ENGINEERING

VIRGINIA POLYTECHNIC INSTITUTE AND STATE UNIVERSITY

BLACKSBURG, VIRGINIA

College of Engineering
VPI & SU
Blacksburg, VA. 24061

VPI-E-77-6 February, 1977

Tensile & Compressive Test Results for Metal Matrix Composites

Mark J. Shuart
Carl T. Herakovich

Department of Engineering Science & Mechanics

NASA-VPI&SU Program in Composite Materials Research and Education

Interim Report: NASA Grant NGR 47-004-129

Prepared for:

Composites Section
Materials Application Branch
NASA-Langley Research Center

BIBLIOGRAPHIC DATA SHEET	1. Report No. VPI-E-77-6	2.	3. Recipient's Accession No.

4. Title and Subtitle

TENSILE AND COMPRESSION TEST RESULTS FOR METAL MATRIX COMPOSITES

5. Report Date: February, 1977

6.

7. Author(s)

Mark J. Shuart and Carl T. Herakovich

8. Performing Organization Rept. No. VPI-E-77-6

9. Performing Organization Name and Address

Virginia Polytechnic Institute and State University
Engineering Science and Mechanics
Blacksburg, Virginia 24061

10. Project/Task/Work Unit No.

11. Contract/Grant No. NGR 47-004-129

12. Sponsoring Organization Name and Address

National Aeronautics & Space Administration
Langley Research Center
Hampton, Virginia 23665

13. Type of Report & Period Covered

14.

15. Supplementary Notes

see page i

16. Abstracts

17. Key Words and Document Analysis. 17a. Descriptors

Metal-matrix composites, Young's Modulus, Poisson's Ratio, ultimate strength, tension, compression, test methods, coupon, sandwich beams

17b. Identifiers/Open-Ended Terms

17c. COSATI Field/Group

18. Availability Statement	19. Security Class (This Report)	21. No. of Pages
Distribution unlimited	UNCLASSIFIED	
	20. Security Class (This Page) UNCLASSIFIED	22. Price

INSTRUCTIONS FOR COMPLETING FORM NTIS-35 (Bibliographic Data Sheet based on COSATI Guidelines to Format Standards for Scientific and Technical Reports Prepared by or for the Federal Government, PB-180 600).

1. **Report Number.** Each individually bound report shall carry a unique alphanumeric designation selected by the performing organization or provided by the sponsoring organization. Use uppercase letters and Arabic numerals only. Examples FASEB-NS-73-87 and FAA-RD-73-09.

2. Leave blank.

3. **Recipient's Accession Number.** Reserved for use by each report recipient.

4. **Title and Subtitle.** Title should indicate clearly and briefly the subject coverage of the report, subordinate subtitle to the main title. When a report is prepared in more than one volume, repeat the primary title, add volume number and include subtitle for the specific volume.

5. **Report Date.** Each report shall carry a date indicating at least month and year. Indicate the basis on which it was selected (e.g., date of issue, date of approval, date of preparation, date published).

6. **Performing Organization Code.** Leave blank.

7. **Author(s).** Give name(s) in conventional order (e.g., John R. Doe, or J.Robert Doe). List author's affiliation if it differs from the performing organization.

8. **Performing Organization Report Number.** Insert if performing organization wishes to assign this number.

9. **Performing Organization Name and Mailing Address.** Give name, street, city, state, and zip code. List no more than two levels of an organizational hierarchy. Display the name of the organization exactly as it should appear in Government indexes such as Government Reports Index (GRI).

10. **Project/Task/Work Unit Number.** Use the project, task and work unit numbers under which the report was prepared.

11. **Contract/Grant Number.** Insert contract or grant number under which report was prepared.

12. **Sponsoring Agency Name and Mailing Address.** Include zip code. Cite main sponsors.

13. **Type of Report and Period Covered.** State interim, final, etc., and, if applicable, inclusive dates.

14. **Sponsoring Agency Code.** Leave blank.

15. **Supplementary Notes.** Enter information not included elsewhere but useful, such as: Prepared in cooperation with . . . Translation of . . . Presented at conference of . . . To be published in . . . Supersedes . . . Supplements . . . Cite availability of related parts, volumes, phases, etc. with report number.

16. **Abstract.** Include a brief (200 words or less) factual summary of the most significant information contained in the report. If the report contains a significant bibliography or literature survey, mention it here.

17. **Key Words and Document Analysis. (a). Descriptors.** Select from the Thesaurus of Engineering and Scientific Terms the proper authorized terms that identify the major concept of the research and are sufficiently specific and precise to be used as index entries for cataloging.
(b). Identifiers and Open-Ended Terms. Use identifiers for project names, code names, equipment designators, etc. Use open-ended terms written in descriptor form for those subjects for which no descriptor exists.
(c). COSATI Field/Group. Field and Group assignments are to be taken from the 1964 COSATI Subject Category List. Since the majority of documents are multidisciplinary in nature, the primary Field/Group assignment(s) will be the specific discipline, area of human endeavor, or type of physical object. The application(s) will be cross-referenced with secondary Field/Group assignments that will follow the primary posting(s).

18. **Distribution Statement.** Denote public releasability, for example "Release unlimited", or limitation for reasons other than security. Cite any availability to the public, other than NTIS, with address, order number and price, if known.

19 & 20. **Security Classification.** Do not submit classified reports to the National Technical Information Service.

21. **Number of Pages.** Insert the total number of pages, including introductory pages, but excluding distribution list, if any.

22. **NTIS Price.** Leave blank.

ABSTRACT

This report presents experimental results of the mechanical behavior of two metal matrix composite systems at room temperature. Ultimate stress, ultimate strain, Poisson's ratio, and initial Young's Modulus are documented for BORSIC/Aluminum in uniaxial tension and Boron/Aluminum in uniaxial tension and compression. A more precise definition of Poisson's ratio is used for nonlinear stress-strain behavior. A comparison of compression results for B/Al as obtained from sandwich beam compression specimens and IITRI coupon compression specimens is presented.

1.0 INTRODUCTION

In order to make optimum use of available materials, a thorough investigation of their mechanical properties is essential. Hence, any new material must be subjected to extensive testing prior to its use. Composite materials are no exception to this rule. Testing continues to be done on many different types of composites under a variety of loading conditions. It is a notable trait of these materials that their design can be tailored to fit the application.

Perhaps a primary reason for the development of metal matrix composite materials has been their ability to combine the properties of metals and fiber-reinforced composites effectively. Indeed, the increased strength and stiffness of resin-matrix composites is well documented; the higher melting point of metals would be a significant addition to these properties. Thus, metal matrix composites offer added stiffness and strength with a possible increase in useful temperature range over that of resin-matrix composites.

This report is a preliminary study of the tensile and compressive behavior of two metal matrix composites (Boron/Aluminum and BORSIC[1]/Aluminum) at room temperature. Ultimate stress, ultimate strain, Poisson's ratio, and initial Young's Modulus are documented for BORSIC/Aluminum in uniaxial tension and Boron/Aluminum in uniaxial tension and uniaxial compression. Two different compressive testing techniques were used: (1) a sandwich beam in four-point bending, and (2) the IITRI compression test [1]. This report also compares these two methods.

2.0 EXPERIMENTAL PROGRAM

2.1 *Materials*

The Boron/Aluminum system (B/Al) combines 5.6 mil boron fibers and

---

1 Registered tradename

6061 aluminum matrix[2]. The BORSIC/Aluminum system (Bsc/Al) consists of 5.7 mil silicon-carbide coated boron fibers and 6061 aluminum matrix.

The tension specimens used for both systems were nominally 10" in length and 0.75" in width. Except as noted, two fiberglass end tabs, 2.5" long, were bonded to each end resulting in a 5" test section. Three different laminate orientations consisting of eight plies were tested for Bsc/Al. B/Al properties were obtained for six different orientations where one orientation has six plies and the others have eight plies.

Two compression specimens were used for the B/Al system as pictured in Figure 1. The sandwich beam specimen has nominal dimensions of 22" in length, 1" in width, and 1.5" between the flanges. The top flange has the 4" composite test section which is loaded in compression using four-point bending (Figure 2). The bottom flange is titanium. Five different laminates of constant ply thickness were tested. The IITRI specimens were cut from the composite flange of the sandwich beam specimen as indicated in Figure 1. The IITRI specimens measured approximately 4.25" in length and 0.25" in width. Two fiberglass end tabs, 2.0" long, were bonded to each end of the coupon resulting in a 0.25" test section. Since these coupons are taken from the sandwich beam, the same five laminate orientations as the beam were tested.

Table 1 lists material systems, laminate configurations, and nominal specimen thicknesses for each type of test.

2.2 *Preliminary Investigation*

As an introduction, a search for published constituent material properties of the Bsc/Al system was conducted. This system has exhibited better elevated temperature properties than B/Al. Surprisingly, the

---

[2] This report is a continuation of the work of Mr. C. N. Viswanathan and duplicates his specimen geometry [2].

search indicated that the constituent material properties are not well documented. It was found that the aluminum used as the matrix material is initially in an F condition. This is a general condition representing the as-fabricated state. Because of this classification no exact material properties are available. Hence, very generalized aluminum properties have been used to characterize the matrix behavior. However, the use of these properties disregards any possible effects on the metal of the diffusion-bonding process for fabricating the composite. This fabrication procedure could result in the matrix being stronger and/or tougher due to the nature of cooling after bonding.

Further difficulties were encountered with gathering fiber properties. In this case, the infancy of the BORSIC fiber proved to be the drawback. Also, data were often unavailable regarding the temperature dependent nature of the properties.

All available properties are presented in Table 2.

2.3 *Test Equipment*

The uniaxial tension tests for both the B/Al and Bsc/Al systems were performed at NASA/Langley Research Center. The uniaxial compression test utilizing the sandwich beam in four-point bending was also performed at NASA/Langley, but the IITRI-type compression tests were performed at VPI & SU.

All tests at NASA/Langley used the 120 kip Tinius-Olson testing machine with a constant load rate to failure. Foil-type strain gages measured strain which was recorded using the Beckman automatic data acquisition system. The tension tests for the $[0_8]$, $[90_8]$, $[(0/90)_2]_s$ fiber orientations (in both material systems) had longitudinal and transverse strain gages on each side of the specimen. The $[0/\pm45]_s$,

$[+45/(-45)_2/+45]_s$, $[(\pm 30)_2]_s$ configurations had strain rosettes oriented at 0°, 45°, and 90° with the longitudinal axis on either side of the test specimen. The sandwich beams with B/Al flanges oriented at $[0_4]$, $[90_8]$, $[(0/90)_2]_s$ had longitudinal and transverse strain gages on the composite flange only. Further, strain rosettes oriented at 0°, 45°, and 90° with the longitudinal axis were located on this flange for the $[(\pm 30)_2]_s$ and $[+45/(-45)_2/+45]_s$ laminates.

The tests at VPI & SU used the Instron model 1125 testing machine. Laminates were tested using a monotonically increasing load to failure under constant head rate. Strains were automatically recorded from the foil-type gages using the CB^2 data acquisition system [3]. Every specimen had a longitudinal gage on each side and a transverse gage on just one side.

3.0 TEST RESULTS

3.1 *BORSIC/Aluminum System*

As previously mentioned, this system was tested in uniaxial tension. The results for ultimate stress, ultimate longitudinal strain, ultimate transverse strain, initial Young's Modulus, and range of Poisson's ratio are presented in Table 3. Poisson's ratio has been defined as the change in lateral strain for a change in axial strain [4]. It is assumed to be constant during each increment of strain. All end tabs were bonded to the specimens using contact cement. No stress-strain curves are included for any of the tests performed in this study since they essentially duplicate previous results [2].

The $[+45/(-45)_2/+45]_S$ orientation was found to be incorrectly fabricated for tension specimens of both material systems. During testing of these laminates, the characteristic twisting of an unsymmetric

laminate occurred. A portion of a failed specimen was subsequently bathed in a sodium hydroxide solution to leach out the aluminum matrix. This revealed the true specimen orientation, $[+45/(-45)_2/(+55)_2/(-45)_2/+55]$. This configuration was also verified by X-ray. Thus, the reported data are unreliable for the $[+45/(-45)_2/\mp45]_s$ orientation.

3.2 *Boron/Aluminum System*

3.2.1 Tension specimens

The data for the B/Al uniaxial tension tests are assembled in Table 4. Three specimens having a $[0_8]$ orientation were tested, but only two specimens were tested for other orientations.

Some variation in method of load introduction was performed on the $[0_8]$ coupons. The first coupon utilized contact cement for bonding the end tabs to the specimen. Because the contact cement was unable to maintain the bond between end tabs and specimen during Bsc/Al tests, one specimen had tabs bonded with 934 adhesive[3]. This adhesive does require a 200°F cure cycle. The final $[0_8]$ coupon did not use end tabs at all. A fine emory paper was used between the specimen and the grips of the test machine. Surprisingly, the data from these three tests are inconclusive as to tab influence. Moreover, the necessity of end tabs is questionable for this material. Nevertheless, end tabs were used on all additional tensile specimens. Contact cement was used because of its ease in bonding.

Another testing technique used on these coupons was to grip the end tabs approximately 1/2" behind the beginning of the taper. Several specimens were previously observed to fail in or near the gripped region, an area of stress concentration. It was believed that by gripping

---

[3] Product of Dexter Corporation

farther back on the end tab, the load would be more uniformly introduced into the composite. However, several of the specimens tested were still found to fail in the vicinity of the gripped region. There was no correlation between ultimate stress and failure location. Hence, it would be questionable to attribute all these failures to local stress concentrations because several failures did occur well into the test section.

3.2.2 Sandwich beam compression specimens

Table 5 presents the B/Al compression data for the sandwich beam specimens. Once again, two specimens were tested for each orientation except the $[0_4]$ laminate; three specimens were tested for this case.

A variation in method of load application was used for the $[0_4]$ laminates. The points of the test fixture that introduce load to the composite flange of the beam could have either a rounded or flat surface. The first $[0_4]$ specimen was tested with the load applied through the rounded surface. This caused a significant amount of bearing stress on the particular load points. In order to introduce the load over a larger area, the flat surface of the test fixutre was used to load the last two $[0_4]$ specimens. A typical failure using the flat surface is shown in Figure 3. Perhaps a further suggestion to decrease bearing stress would be to use small pads under the load points [5].

The cause of failure in the $[90_8]$ specimens was buckling (Figures 4 and 5). Hence, the ultimate compressive values for these tests may not correspond to the true maximum compressive values of this material. A $[(0/90)_2]_S$ sandwich beam is shown in Figure 6; its failure surface was much more abrupt than the $[0_4]$ specimen, and buckling was minimal compared to the $[90_8]$ orientation. The $[(\pm 30)_2]_S$ specimen failed in its characteristic manner (Figure 7), along a line oriented at 30° with the longitudinal

axis of the beam. The $[+45/(-45)_2/+45]_S$ beam was not tested to failure in compression. The large strains that accompanied the application of load caused the beam to contact the bottom of the test fixture before the ultimate stress was reached. Further, these large strains exceeded the maximum values for the data acquisition system. Hence, the reported values of ultimate strain for this orientation correspond to the maximum readable strains during the test (Table 5). The second test of this orientation was a tension test. The failure surface for this test is shown in Figure 8; the curvature of the beam indicates the degree of strain.

3.2.2 IITRI Compression Specimens

The compression data for the B/Al IITRI specimen are presented in Table 6. Four specimens were tested for each orientation except the $[(0/90)_2]_s$; two laminates were tested for this configuration.

The failure surface of a $[0_4]$ laminate is shown in Figure 9. The failure was catastrophic and characteristic of compressive loading. The $[90_8]$ specimens buckled as pictured in Figure 10. Thus, for a $[90_8]$ laminate the maximum compressive values for the IITRI test do not correspond to the true compressive strength of the material. Similar behavior for this fiber orientation was noted in the sandwich beam test. The $[(0/90)_2]_s$ configuration has a failure surface that appears to combine $[0_4]$ and $[90_8]$ failure modes. The $[(0/90)_2]_s$ specimen in Figure 11 illustrates a smaller amount of buckling when compared to a $[90_8]$ surface and a contribution from fiber breakage, characteristic of the $[0_4]$ failure.

The $[(\pm 30)_2]_s$ and $[+45/(-45)_2/+45]_s$ specimens exhibit very similar behavior (Figures 12 and 13, respectively). The test section of each laminate experiences large transverse strain. This is somewhat expected

due to the higher Poisson's ratio of some angle-ply laminates. Figure 13 clearly shows that the transverse strains are restricted by the gripping influence; this will be discussed further in a following section of this report.

4.0 DISCUSSION

4.1 *Analytical Correlation*

Laminate theory can be used to predict elastic material properties. For a symmetric laminate of thickness 2H, the average in-plane stresses, $\{\bar{\sigma}\}$, can be expressed in terms of the forces per unit length $\{N\}$, as

$$\begin{Bmatrix} \bar{\sigma}_x \\ \bar{\sigma}_y \\ \bar{\tau}_{xy} \end{Bmatrix} = \frac{1}{2H} \begin{Bmatrix} N_x \\ N_y \\ N_{xy} \end{Bmatrix} , \tag{1}$$

or in terms of the midplane strains $\{\varepsilon^\circ\}$,

$$\begin{Bmatrix} \bar{\sigma}_x \\ \bar{\sigma}_y \\ \bar{\tau}_{xy} \end{Bmatrix} = \frac{1}{2H} [A] \begin{Bmatrix} \varepsilon^\circ_x \\ \varepsilon^\circ_y \\ \gamma^\circ_{xy} \end{Bmatrix} , \tag{2}$$

Inverting Eqn. (2) gives midplane strains in terms of the stresses,

$$\{\varepsilon^\circ\} = [a^*]\{\bar{\sigma}\} , \tag{3}$$

where

$$[a^*] = 2H[A]^{-1} . \tag{4}$$

Hence, the elastic properties for the total laminate can be expressed as,

$$E_x = \frac{\bar{\sigma}_x}{\varepsilon^\circ_x} = \frac{1}{a^*_{11}} \; ; \; \nu_{xy} = \frac{-\varepsilon^\circ_y}{\varepsilon^\circ_x} = \frac{-a^*_{12}}{a^*_{11}} . \tag{5}$$

Table 7 compares analytical and experimental values of Young's Modulus and Poisson's ratio (elastic range) for the B/Al system. The $[0_4]$ and $[90_8]$ laminates are included and their properties are input for further calculation. The $[(0/90)_2]_s$ laminate properties follow rule of mixtures calculations using $[0_4]$ and $[90_8]$ input. Upon inspection of the table, it is seen that the predicted modulii are greater than experimental modulii except for the $[(0/90)_2]_s$ IITRI compresssion case. Further, the predicted Poisson's ratios are smaller than the experimental values except for the $[(0/90)_2]_s$ tension case. The discrepancies between experimental and analytical values may be explained by matrix yielding caused by residual thermal stresses [6].

4.2 *Poisson's Ratio Data*

As previously stated, Poisson's ratio is defined as the change in lateral strain divided by the change in axial strain [4], i.e.

$$\nu_{xy} = \frac{-d\varepsilon_y}{d\varepsilon_x} \quad . \tag{6}$$

The values presented in this report were obtained by plotting curves of lateral strain verses axial strain. Poisson's ratio is then taken to be the slope of a curve at selected intervals. Figures 14-24 illustrate such curves for tension and compression tests (curves for some tests are not included as strain gage or data acquisition malfunctions resulted in irrelevent data).

Several trends are apparent in the Poisson's ratio curves. The $[0_8]$ plots (Figure 14) are bilinear with the knee occurring approximately at the proportional limit of the aluminum matrix [7]. The $[90_8]$ specimens are characterized by curves (Figures 15 and 21) that quickly attain a maximum followed by a negative Poisson's ratio, i.e. there is lateral expansion associated with an axial expansion. This negative ratio may

be the result of a failure mechanism in the matrix material. This behavior is not completely consistent with the $[90_8]$ IITRI coupons. These tests terminated at much lower axial strain levels. The curves for the $[(0/90)_2]_s$ laminates (Figures 16 and 22) have a slope that becomes erratic and decreases in magnitude prior to failure. As expected, this laminate exhibits behavior that combines [0°] and [90°] behavior. The $[+45/(-45)_2/+45]_s$ specimens exhibit a small increase in Poisson's ratio throughout each test (Figures 17 and 23). It is interesting to note that the change in lateral strain is very close to the change in axial strain for this configuration with Poisson's ratio approximately equal to unity throughout the test. The slope of the $[0/\pm45]_s$ curve (Figure 18) increases throughout the test (typical of the $[+45/(-45)_2/+45]_s$), and the Poisson's ratio values lie between the $[0_8]$ and $[+45/(-45)_2/+45]_s$ laminates, as expected. The $[(\pm30_2)]_s$ laminates (Figures 19 and 24) have the highest Poisson's ratios. The values are steadily increasing throughout each test with ratios greater than 2.0 being often attained.

Another trend is that the Poisson's ratios for the Bsc/Al laminates are slightly larger than the corresponding B/Al laminates. This may be attributed to the larger, 5.7 mil., fiber used in the Bsc/Al system.

4.3 *Comparison of Compressive Test Techniques*

From the standpoint of static analysis, both the beam and the coupon experience compressive loading in their test sections. However, other constraints inherent in each specimen geometry can obscure meaningful results.

The sandwich beam is constructed of two flanges and a honeycomb core. This honeycomb is bonded to each flange and may influence any lateral behavior in the test section. It would follow that a decrease

in lateral strain would result in a higher apparent Young's Modulus and a lower apparent Poisson's ratio when compared to corresponding values of the IITRI test. However, this pattern is not illustrated in all the data. Although the $[0_4]$ and $[90_8]$ laminates exhibit higher modulii from beam tests than from coupons, other laminates do not portray similar trends.

The IITRI coupon has an extremely small test section (0.25"). This section becomes critical when applying St. Venant's principle. The proximity of the tabs and machine grips to the test region may have significant effect on the data. Indeed, the $[(\pm 30)_2]_s$ and $[+45/(-45)_2/+45]_s$ orientations have large lateral deformations (Figures 12 and 13, respectively). Also, these deformations continue into the gripped region of the specimen. Hence, it is very likely that the deformations are experiencing some grip effect. Obviously, for the $[+45/(-45)_2/+45]_s$ laminate (Figure 13) the requirement of loading far-removed from the test section is not met.

If the state of stress is not uniform throughout the test section, the Poisson's ratio data becomes questionable. Figure 25 shows the strain gage locations on a typical IITRI specimen. The lateral gage is located on the far right of the test area, and the axial gage is located close to the middle. Poisson's ratio has been defined as a coupling of lateral and axial strains at a point. Because of the different strain gage locations, it is apparent that the lateral strain (at least for some laminates) may not be solely the result of the axial strain. It may also be a function of machine gripping constraint. A better test procedure would be to use stacked strain gages that measure strains in the same region.

Another consideration for these IITRI tests is the load history of

each compression coupon. As shown in Figure 1, the coupons are cut from the composite flange of the sandwich beam. Calculations reveal that the area of the IITRI coupons experiences half the loading used to fail the sandwich beam during the four-point bending test. However, it has been shown that cycling has a small effect on the elastic properties of Bsc/Al [2]; negligible effects are assumed for this investigation.

Perhaps the most significant comparison between the sandwich beam and the IITRI coupon is the maximum attainable axial strain for each test. It appears that the IITRI coupons experience premature failure for some laminates. This is best illustrated by the $[90_3]$ specimens (Figures 15 and 21). In the tension and four-point bending tests the curves for these laminates attain a maximum transverse strain and then decrease. This maximum is not evident in the IITRI $[90_8]$ tests since failure occurs at lower axial strain levels.

5.0 CONCLUDING REMARKS

This report presents the results of forty-one tension and compression tests on metal matrix composite materials. The more precise definition of Poisson's ratio used in the report extends the meaningful use of this material property into the nonlinear range of material behavior. The reliability of data from some angle-ply IITRI compression tests is questionable. There is significant grip influence when testing laminates with high Poisson's ratio such as the $[+45/(-45)_2/+45]_s$ specimen. Further, the lower axial strain levels of some IITRI compression tests when compared to corresponding sandwich beam data indicate that the IITRI specimen often exhibits early failures.

ACKNOWLEDGEMENT

This work was supported by NASA's Langley Research Center under NASA Grant NGR 47-004-129. Dr. John G. Davis, Jr. was the NASA technical monitor and his help is greatly appreciated.

All Boron/Aluminum IITRI compression tests were performed by Mr. James F. Knauss at VPI&SU. Many thanks are offered for his significant contribution to this work.

Finally, the very tedious typing done by Ms. Frances Carter is gratefully acknowledged.

REFERENCES

1. IIT Research Institute, "Development of Engineering Data on the Mechanical and Physical Properties of Advanced Composite Materials", Technical Report AFML-TR-72-205 - Part I, September, 1972.

2. C. N. Viswanathan, J. G. Davis, and C. T. Herakovich, "Tensile and Compressive Behavior of Borsic/Aluminum Composite Laminates", VPI & SU Report VPI-E-74-7, March, 1974.

3. G. H. Wilson and C. T. Herakovich, "A Microprocessor-Based System for Laboratory Data Acquisition", VPI & SU Report VPI-E-75-11, June, 1975.

4. American Society of Testing Materials, "Standard Method of Test for Poisson's Ratio at Room Temperature", 1976 Annual Book of ASTM Standards, Part 10.

5. Advanced Composites Design Guide, 3rd Edition, Volume 4, Advanced Development Division, AFML, Wright-Patterson AFB, Ohio, January, 1973.

6. J. E. Ramsey, J. P. Waszczak, and F. L. Klouman, "An Investigation of Nonlinear Response of Metal-Matrix Composite Laminates", AIAA/ASME/SAE 16th Structures, Structural Dynamics, and Materials Conference, Denver, CO., May, 1975.

7. Mechanical Behavior of Materials, edited by F. A. McClintock and A. S. Argon, Addison-Wesley Publishing Company, Reading, MA., 1966.

TABLE 1

TEST LAMINATE THICKNESSES

Material (Test)	Orientation	Nominal Thickness, Inches
B_{sc}/Al (Tension)	$[0_8]$	0.060
	$[90_8]$	0.060
	$[+45/(-45)_2/+45]_s$	0.060
B/Al (Tension)	$[0_8]$	0.060
	$[90_8]$	0.060
	$[(0/90)_2]_s$	0.060
	$[0/\pm45]_s$	0.045
	$[+45/(-45)_2/+45]_s$	0.060
	$[(\pm30)_2]_s$	0.060
B/Al (Compression)	$[0_4]$	0.028
	$[90_8]$	0.060
	$[(0/90)_2]_s$	0.060
	$[+45/(-45)_2/+45]_s$	0.060
	$[(\pm30)]_s$	0.060

TABLE 2

B_{sc}/Al CONSTITUENT PROPERTIES

Property	100°F	200°F	300°F	400°F	500°F	600°F	700°F	800°F	900°F	1000°F
E, 10^6 psi	11.0	10.8	10.6	10.4	10.2	10.0	9.6	9.2	9.0	8.6
G, 10^6 psi	3.7	3.6	3.5	3.5	3.4	3.3	3.1	2.8	2.7	2.5
ν	0.34	0.35	0.35	0.34	0.33	0.33	0.33	0.34	0.35	0.35
α, 10^{-6} in/in/°F	12.7	13.0	13.3	13.6	13.8	14.1	14.1	14.1	14.1	14.1

BORSIC FIBER

$E = 58 \times 10^6$ psi $\quad \nu = 0.20$

$G = 24 \times 10^6$ psi $\quad \alpha = 2.7 \times 10^{-6}$ in/in/°F

TABLE 3

B_{sc}/Al TENSION DATA

Orientation	σ_x^u, Ksi	ε_x^u, %	ε_y^u, %	E_x, Msi	ν_{xy}
$[0_8]$	152.87	0.55	0.14	27.61	0.24-0.29
$[0_8]$	153.45	0.56	0.15	31.63	0.24-0.26
$[90_8]$	14.66	0.78	0.002	12.04	0.064, -0.005
$[+45/(-45)_2/+45]_2$	23.88	2.41	1.74	15.49	- [1]

[1] Strain Gage Malfunction

TABLE 4

B/Al TENSION DATA

Orientation	σ_x^u, Ksi	ε_x^u, %	ε_y^u, %	E_x, Msi	ν_{xy}
$[0_8]$	209.0	0.80	0.22	26.60	0.22-0.29
$[0_8]$	193.6	0.82	0.22	25.96	0.23-0.28
$[0_8]$	206.3	0.82	0.22	25.60	0.20-0.27
$[90_8]$	11.33	0.45	0.005	5.60	- [1]
$[90_8]$	15.65	0.63	0.006	9.99	0.12, -0.002
$[(0/90)_2]_s$	116.1	0.83	0.02	15.72	0.06-0.02
$[(0/90)_2]_s$	114.1	0.85	0.01	14.65	0.06-0.01
$[+45/(-45)_2/+45]_s$	24.75	3.99	4.29	12.26	0.83-1.00
$[+45/(-45)_2/+45]_s$	24.39	3.85	3.90	8.59	0.92-1.11
$[0/\pm45]_s$	63.38	0.60	0.31	13.98	0.40-0.60
$[0/\pm45]_s$	79.13	0.75	0.41	14.30	0.40-0.66
$[(\pm30)_2]_s$	81.62	1.66	2.73	14.81	0.95-2.30
$[(\pm30)_2]_s$	77.60	1.38	2.35	20.16	1.17-2.48

[1] Strain Gage Malfunction

[2] Actual Lay-up $[+45/(-45)_2/(+55)_2/(-45)_2/+55]$

TABLE 5

B/Al SANDWICH BEAM COMPRESSION DATA

Orientation	σ_x^u, Ksi	ε_x^u, %	ε_y^u, %	E_x, Msi	ν_{xy}
$[0_4]$	220.0	0.60	0.25	38.67	0.32-0.57
$[0_4]$	287.1	- [1]	0.27	41.47	- [1]
$[0_4]$	448.8	1.10	0.40	40.20	0.29-0.40
$[90_8]$	41.79	3.15	0.03	7.57	0.08, -0.02
$[90_8]$	39.83	2.99	0.05	7.84	0.08, -0.02
$[(0/90)_2]_s$	290.3	1.50	0.16	19.49	0.28-0.07
$[(0/90)_2]_s$	269.0	1.40	0.17	19.63	0.20-0.07
$[+45/(-45)_2/+45]_2$	49.65	6.47	6.06	15.57	0.91
$[+45/(-45)_2/+45]_2$ [2]	47.07	6.54	6.14	9.06	0.83-1.00
$[(\pm 30)_2]_s$	74.03	0.81	1.39	25.80	1.17-2.20
$[(\pm 30)_2]_s$	71.69	0.91	2.48	23.62	0.98-4.47

[1] Strain Gage Malfunction

[2] Tension Test

TABLE 6

B/Al IITRI COMPRESSION DATA

Orientation	σ_x^u, Ksi	ε_x^u, %	ε_y^u, %	E_x, Msi	ν_{xy}
$[0_4]$	254.8	1.13	0.32	20.80	0.49-0.72
$[0_4]$	284.2	0.85	0.31	28.87	0.22-0.56
$[0_4]$	261.7	0.84	0.50	27.40	0.23-0.27
$[90_8]$	32.84	1.18	0.05	9.39	0.08-0.02
$[90_8]$	36.06	0.73	0.06	10.25	0.15-0.05
$[(0/90)_2]_s$	227.6	1.03	0.20	19.05	0.36-0.14
$[(0/90)_2]_s$	241.0	1.18	0.22	20.17	0.29-0.22
$[+45/(-45)_2/+45]_s$	25.64	0.73	- [1]	10.00	- [1]
$[+45/(-45)_2/+45]_s$	61.83	0.82	0.58	16.66	0.81
$[(\pm 30)_2]_s$	36.64	0.53	0.73	17.73	0.74-0.25
$[(\pm 30)_2]_s$	47.72	0.51	0.80	19.01	1.40-1.65
$[(\pm 30)_2]_s$	50.64	0.52	0.61	18.46	1.10-1.73
$[(\pm 30)_2]_s$	47.71	0.59	0.92	18.38	0.50-2.95

[1] Strain Gage Malfunction

TABLE 7

COMPARISON OF PREDICTED AND EXPERIMENTAL ELASTIC PROPERTIES

Orientation (type of test)	E_x, Msi Predicted	E_x, Msi Experiment	ν_{xy} Predicted	ν_{xy} Experiment
$[0_8]$ (Tension)	-	26.05	-	0.22
$[0_4]$ (Sandwich Beam Compression)	-	40.11	-	0.31
$[0_4]$ (IITRI Compression)	-	25.69	-	0.31
$[90_8]$ (Tension)	-	7.75	-	-
$[90_8]$ (Sandwich Beam Compression)	-	7.71	-	-
$[90_8]$ (IITRI Compression)	-	9.82	-	-
$[(0/90)_2]_s$ (Tension)	17.0	15.2	0.10	0.06
$[(0/90)_2]_s$ (Sandwich Beam Compression)	24.1	19.6	0.10	0.28
$[(0/90)_2]_s$ (IITRI Compression)	17.9	19.6	0.17	0.33
$[+45/(-45)_2/+45]_s$ [1] (Tension)	14.7	10.4	0.16	0.88
$[+45/(-45)_2/+45]_s$ (Sandwich Beam Compression)	18.0	15.6	0.33	0.91
$[+45/(-45)_2/+45]_s$ (IITRI Compression)	16.7	13.3	0.23	0.81
$[0/\pm45]_s$ (Tension)	19.2	14.0	0.17	0.40
$[(\pm30)_2]_s$ (Tension)	20.6	17.5	0.20	1.06
$[(\pm30)_2]_s$ (Sandwich Beam Compression)	27.1	24.7	0.43	1.07
$[(\pm30)_2]_s$ (IITRI Compression)	20.9	18.4	0.28	0.94

[1] Actual Lay-up $(+45/(-45)_2/(+55)_2/(-45)_2/+55]$

NOTE: B/Al data used for tension tests.

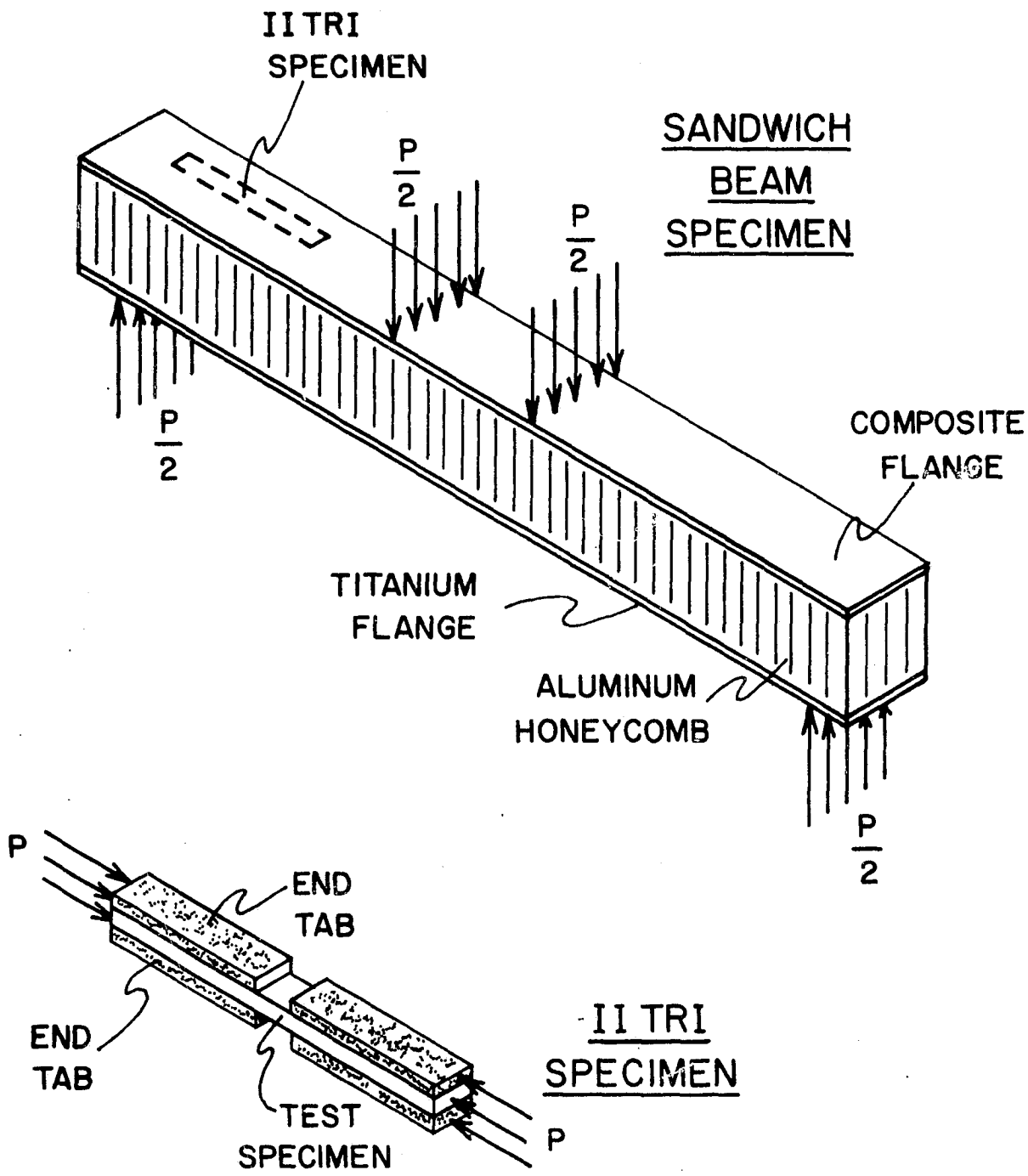

Figure 1. COMPRESSION SPECIMENS

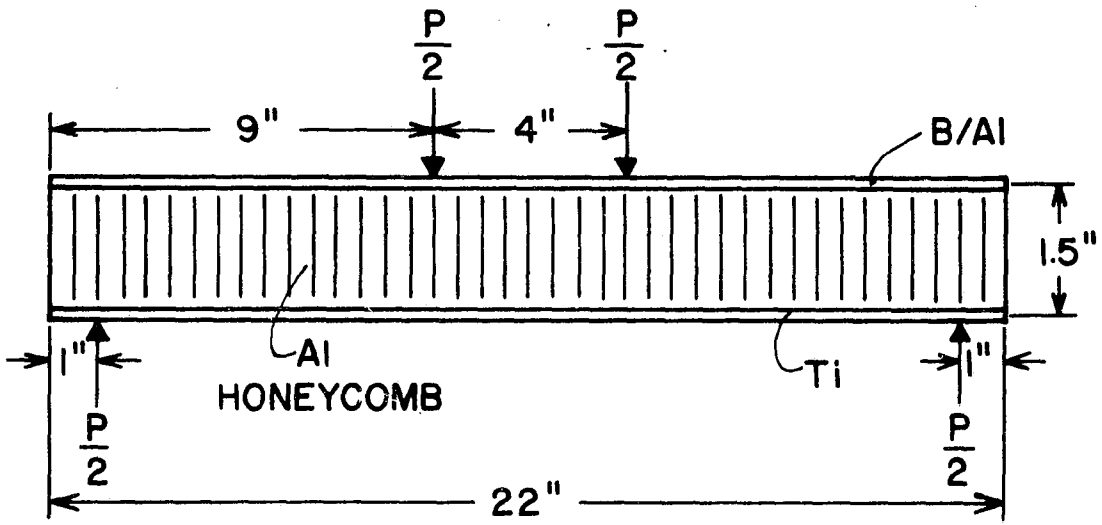

Figure 2. LOADING FOR SANDWICH BEAM COMPRESSION TESTS

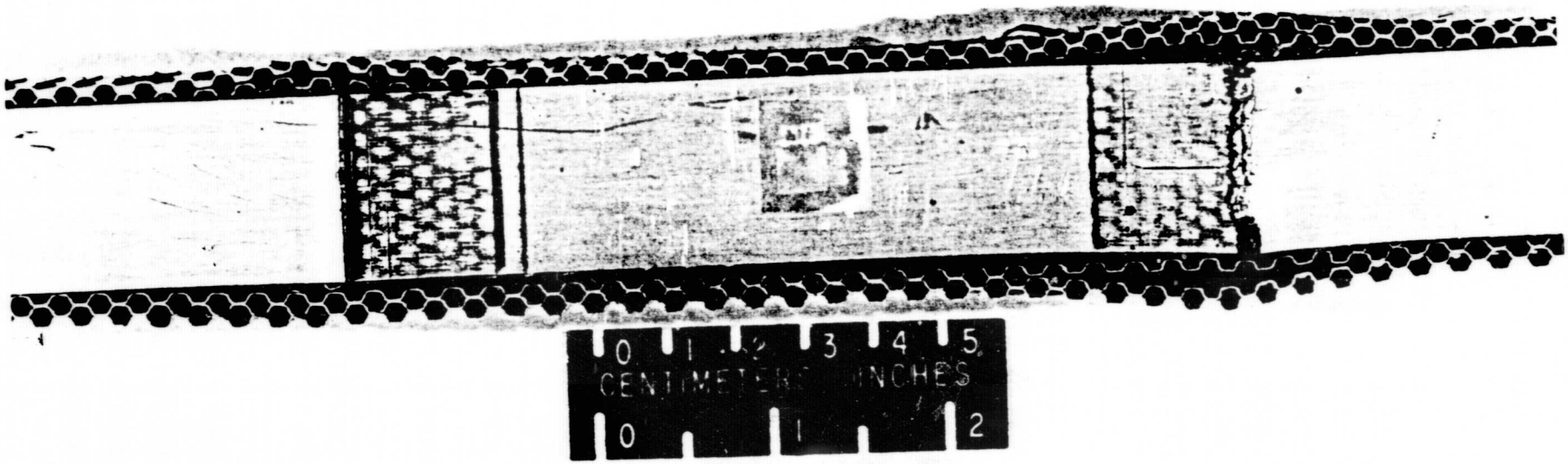

Figure 3. FAILURE SURFACE FOR A $[0_4]$ SANDWICH BEAM COMPRESSION TEST

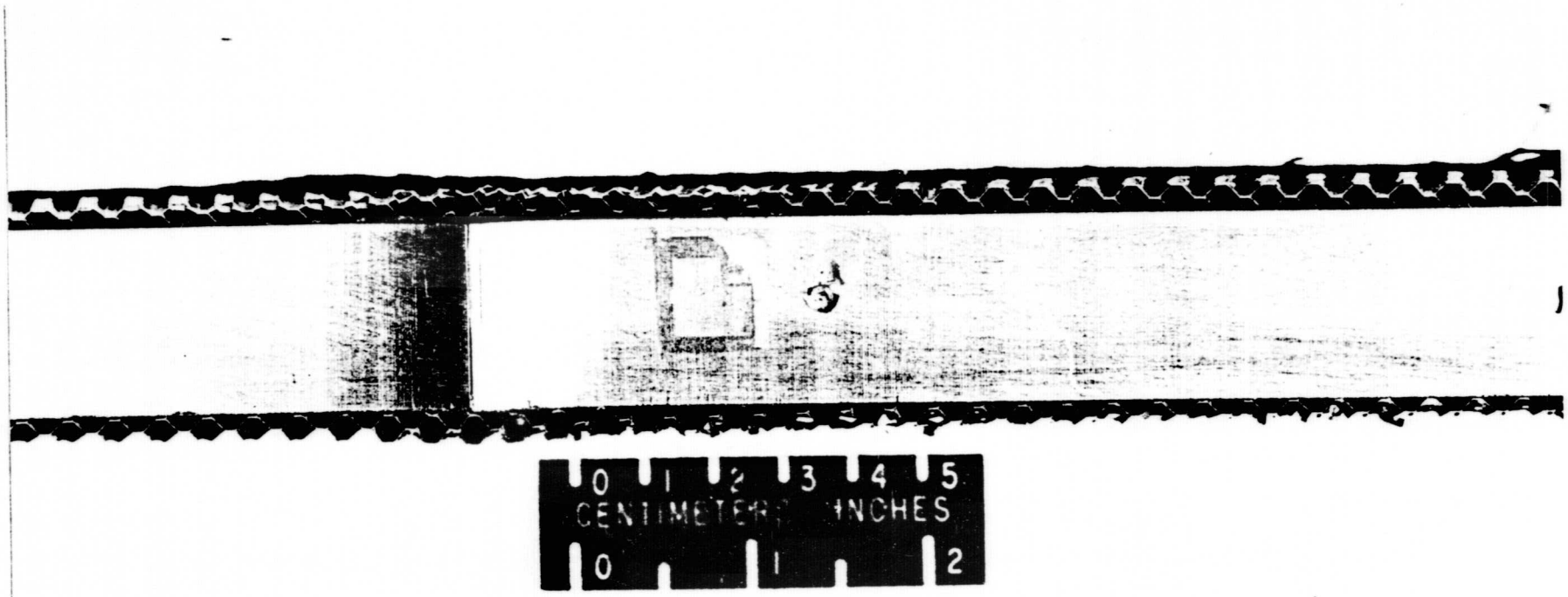

Figure 4. TOP VIEW OF FAILURE SURFACE FOR A $[90_8]$ SANDWICH BEAM COMPRESSION TEST

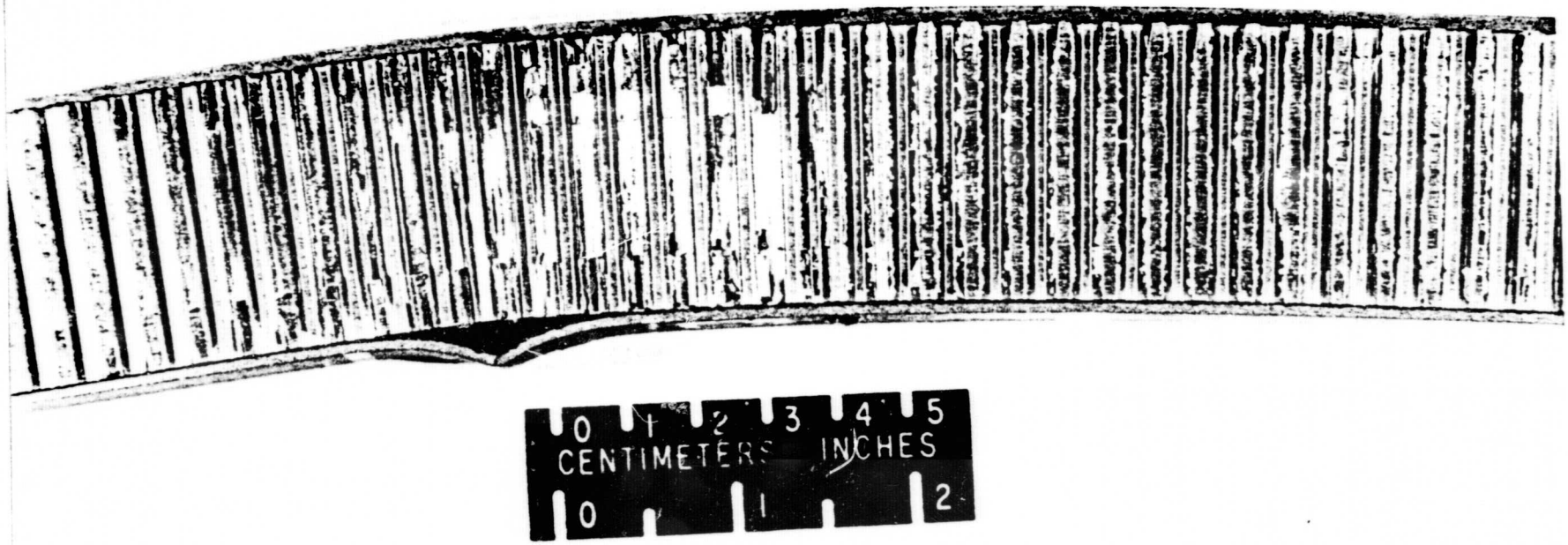

Figure 5. SIDE VIEW OF FAILURE SURFACE FOR A $[90_8]$ SANDWICH BEAM COMPRESSION TEST

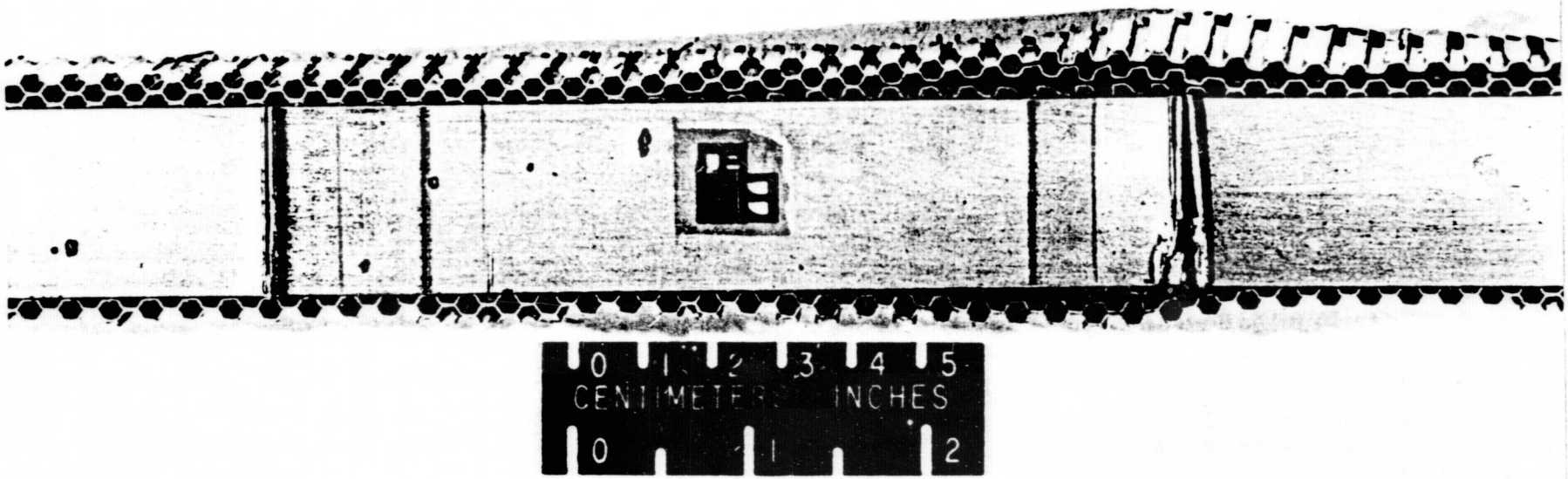

Figure 6. FAILURE SURFACE FOR A $[(0/90)_2]_s$ SANDWICH BEAM COMPRESSION TEST

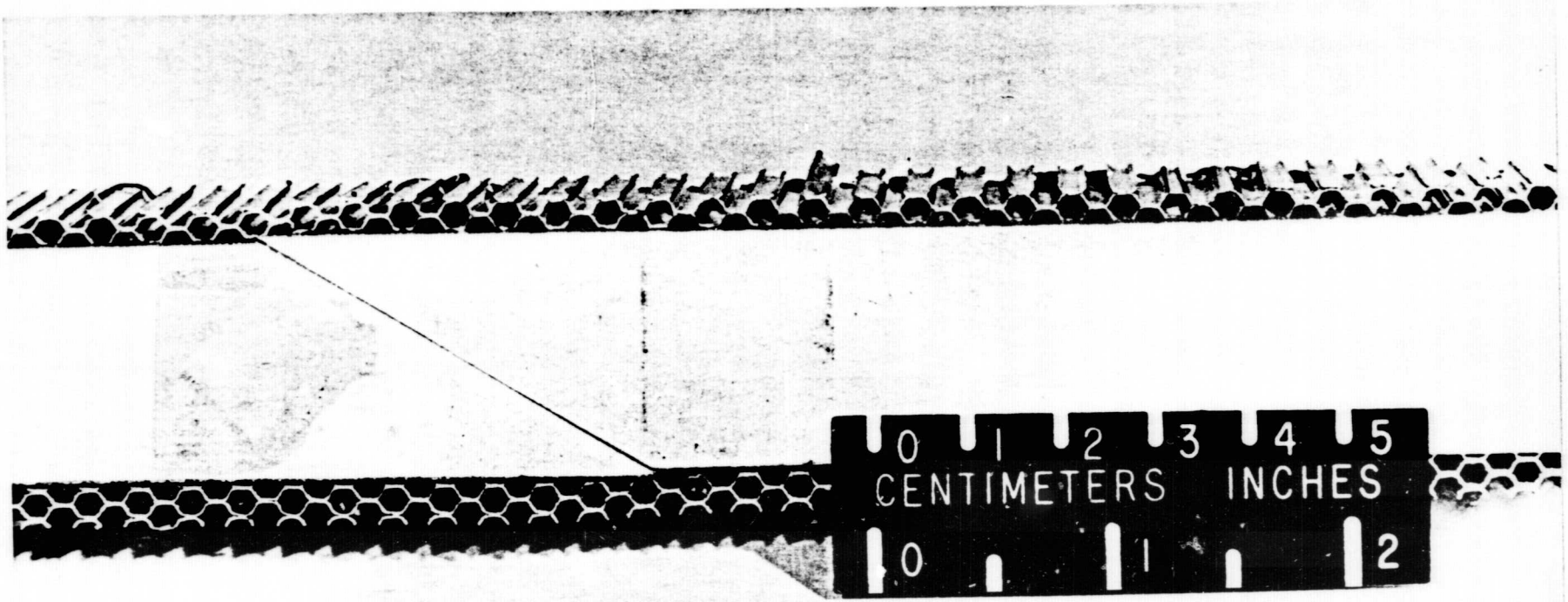

Figure 7. FAILURE SURFACE FOR A $[(\pm 30)_2]_s$ SANDWICH BEAM COMPRESSION TEST

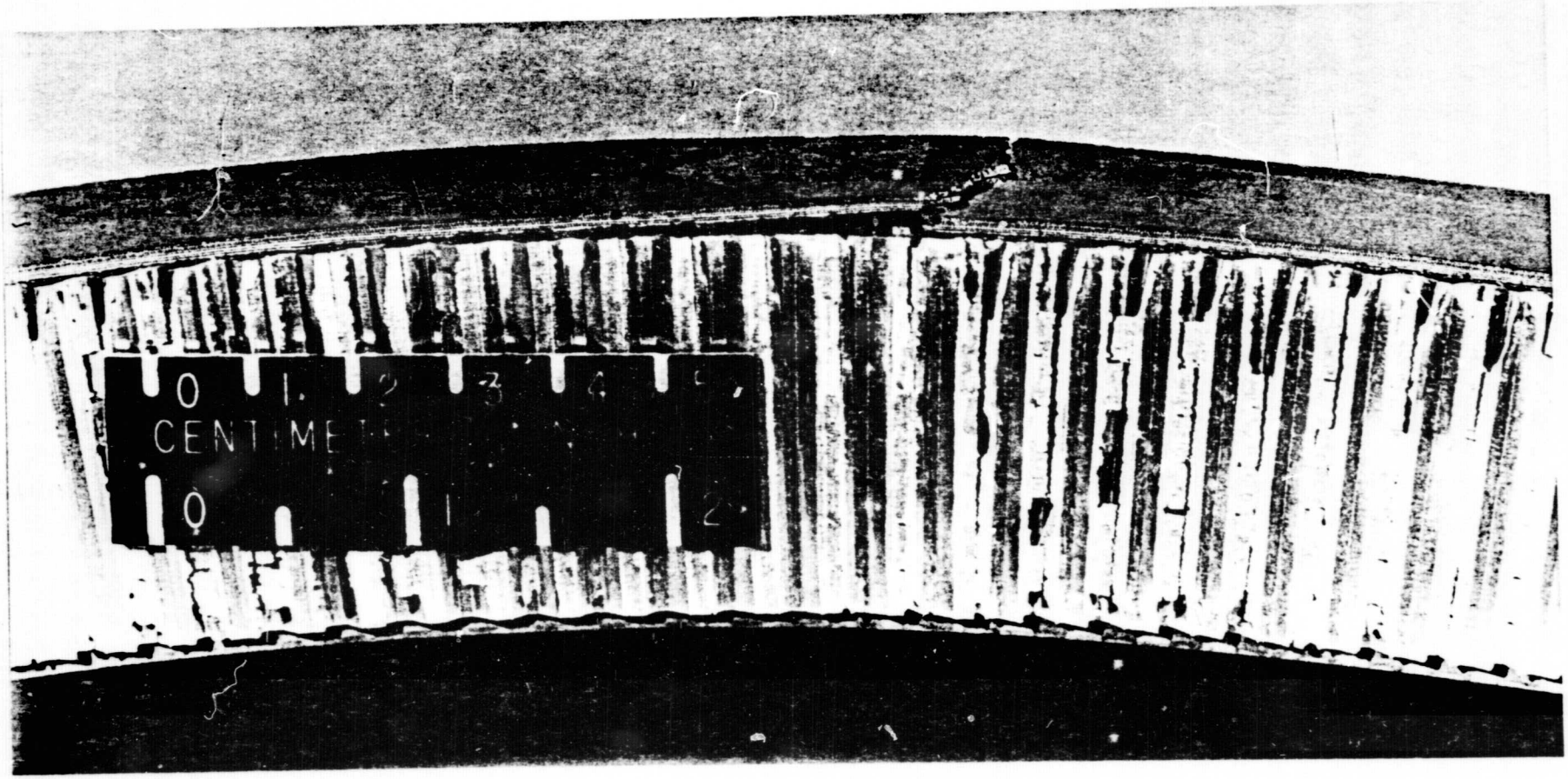

Figure 8. FAILURE SURFACE FOR A $[+45/(-45)_2/+45]_s$ SANDWICH BEAM TENSION TEST

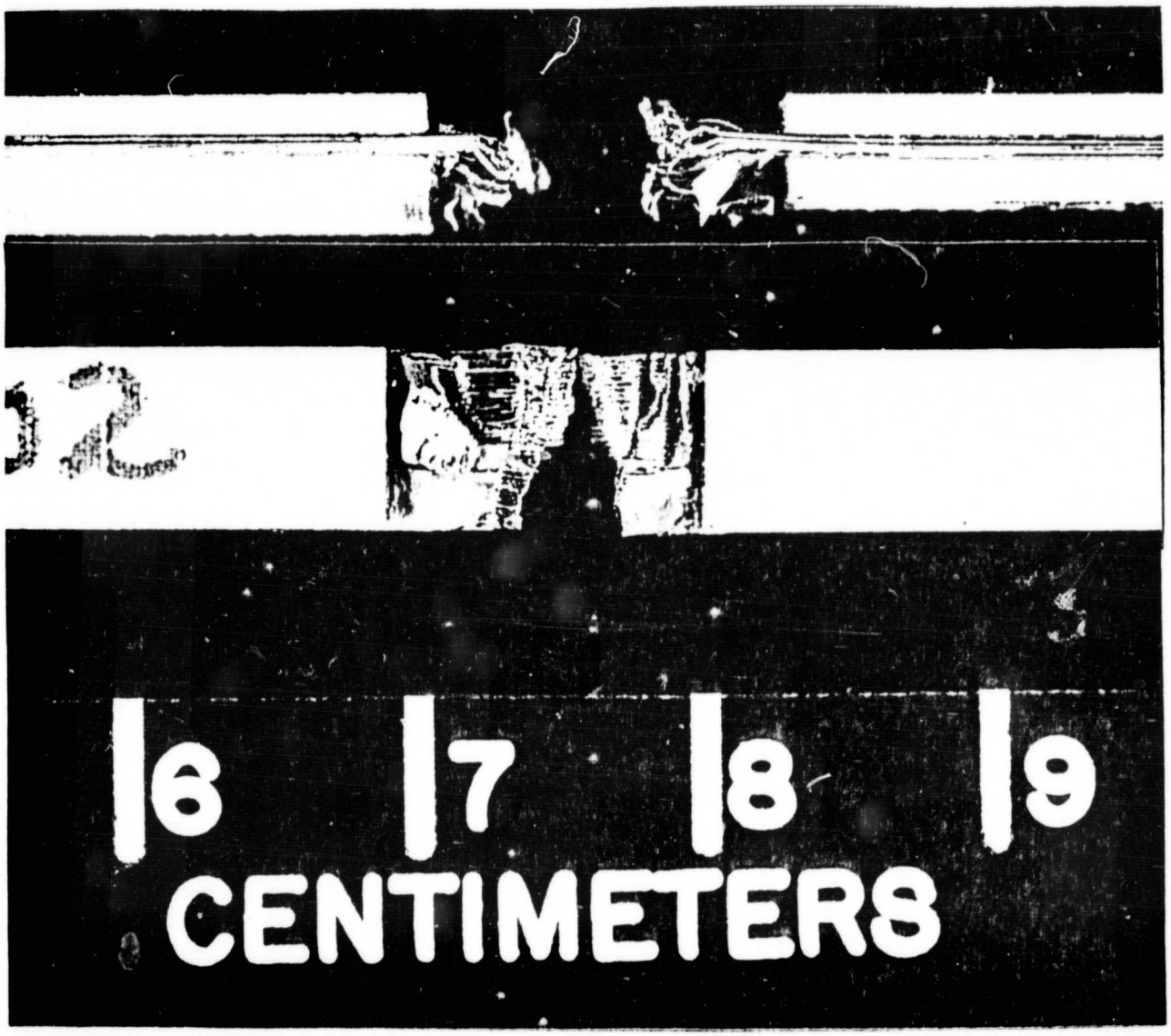

Figure 9. FAILURE SURFACE FOR A $[0_4]$ IITRI COMPRESSION TEST

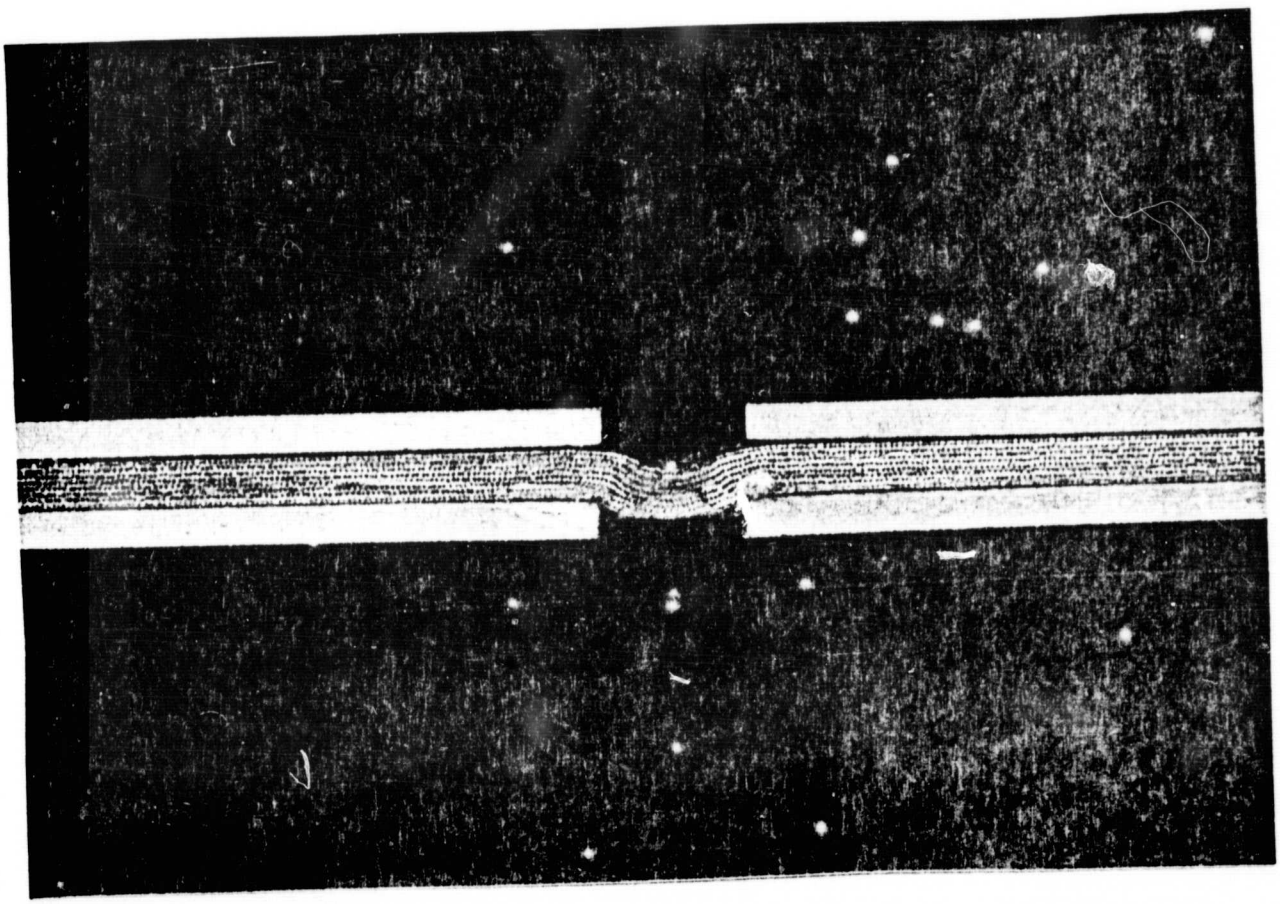

Figure 10. FAILURE SURFACE FOR A $[90_8]$ IITRI COMPRESSION TEST

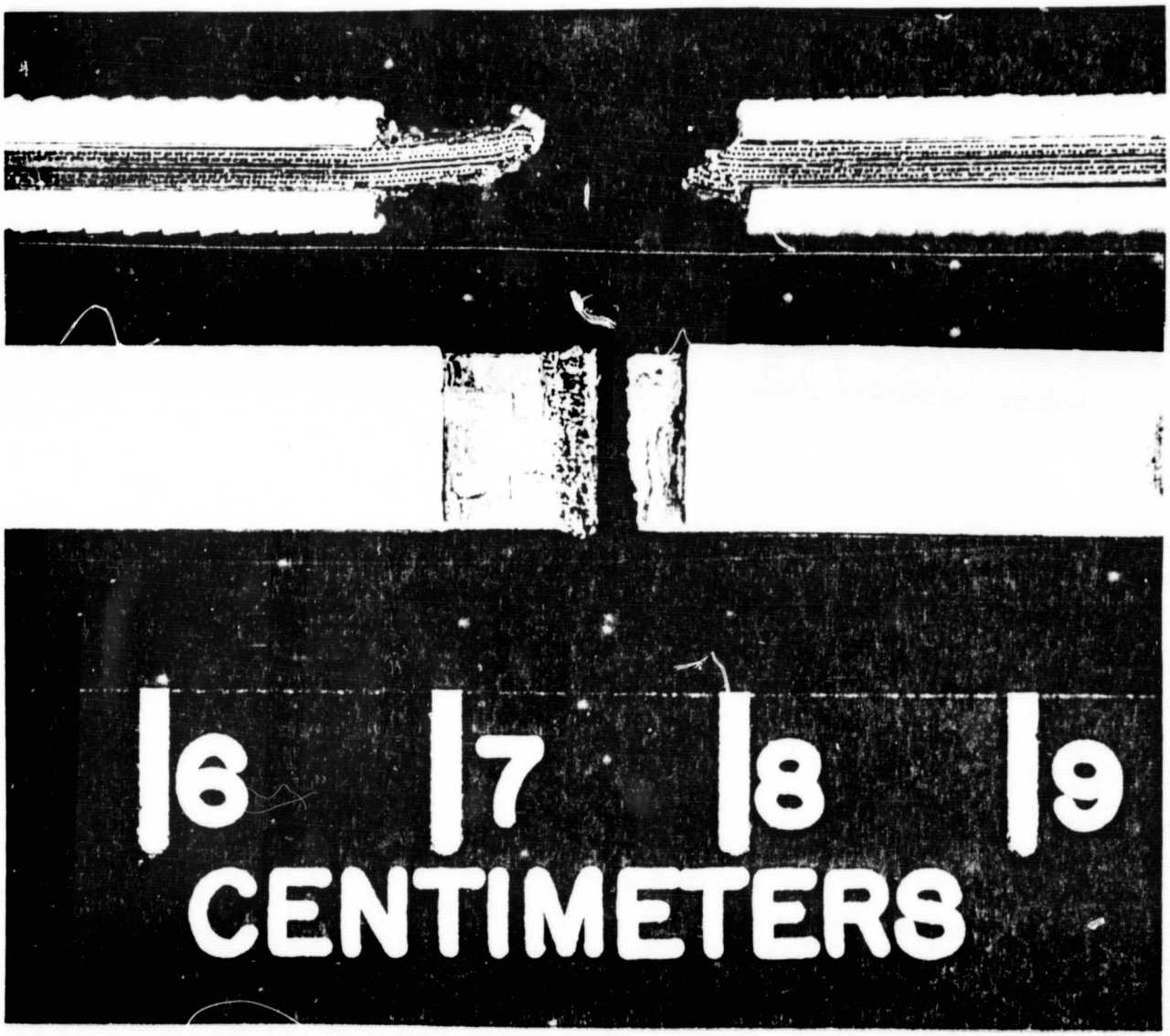

Figure 11. FAILURE SURFACE FOR A $[(0/90)_2]_s$
IITRI COMPRESSION TEST

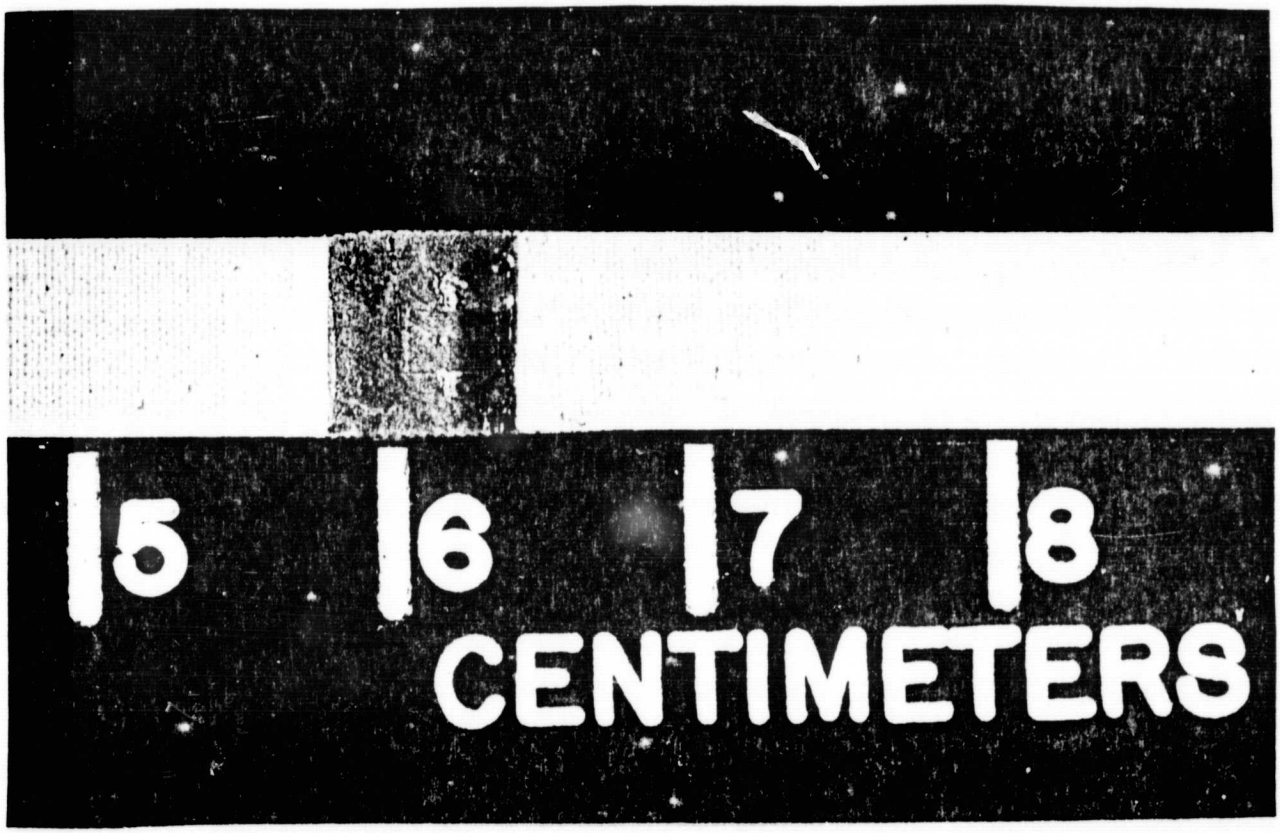

Figure 12. FAILURE SURFACE FOR A $[(\pm 30)_2]_s$
IITRI Compression Test

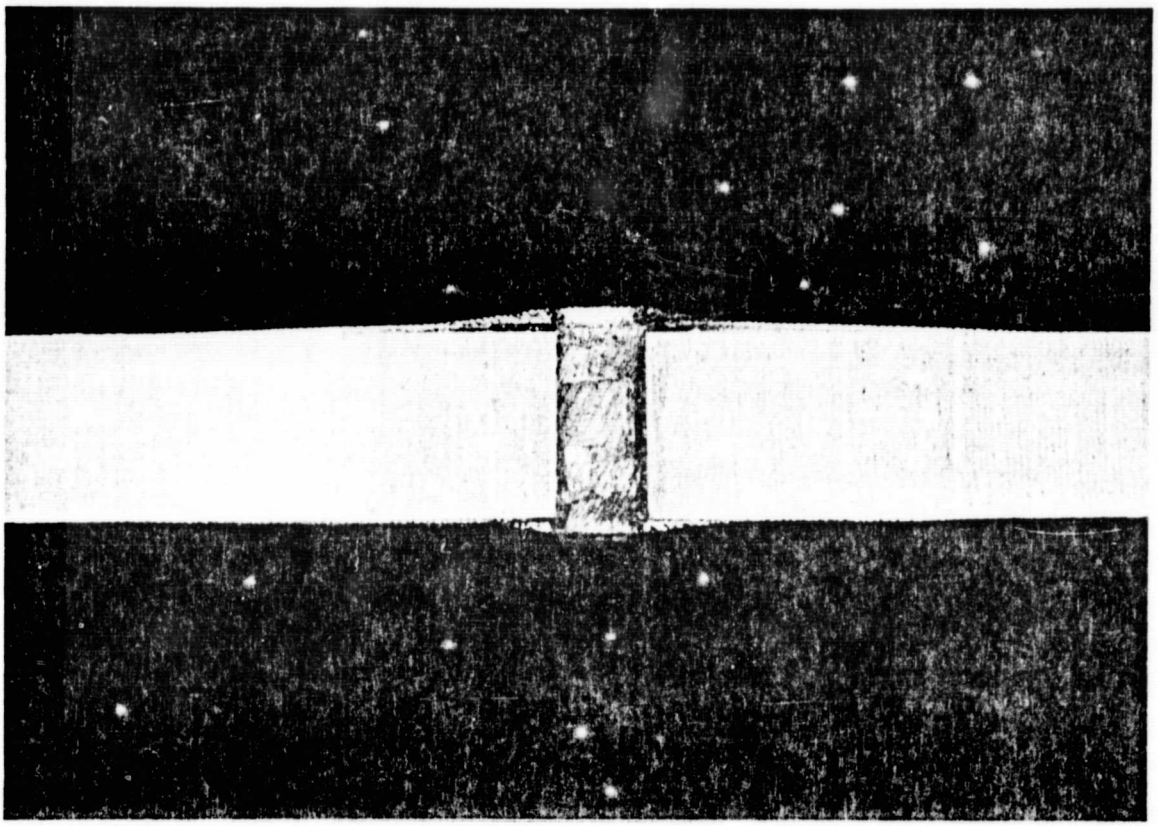

Figure 13. FAILURE SURFACE FOR A $[+45/(-45)_2/+45]_s$
IITRI COMPRESSION TEST

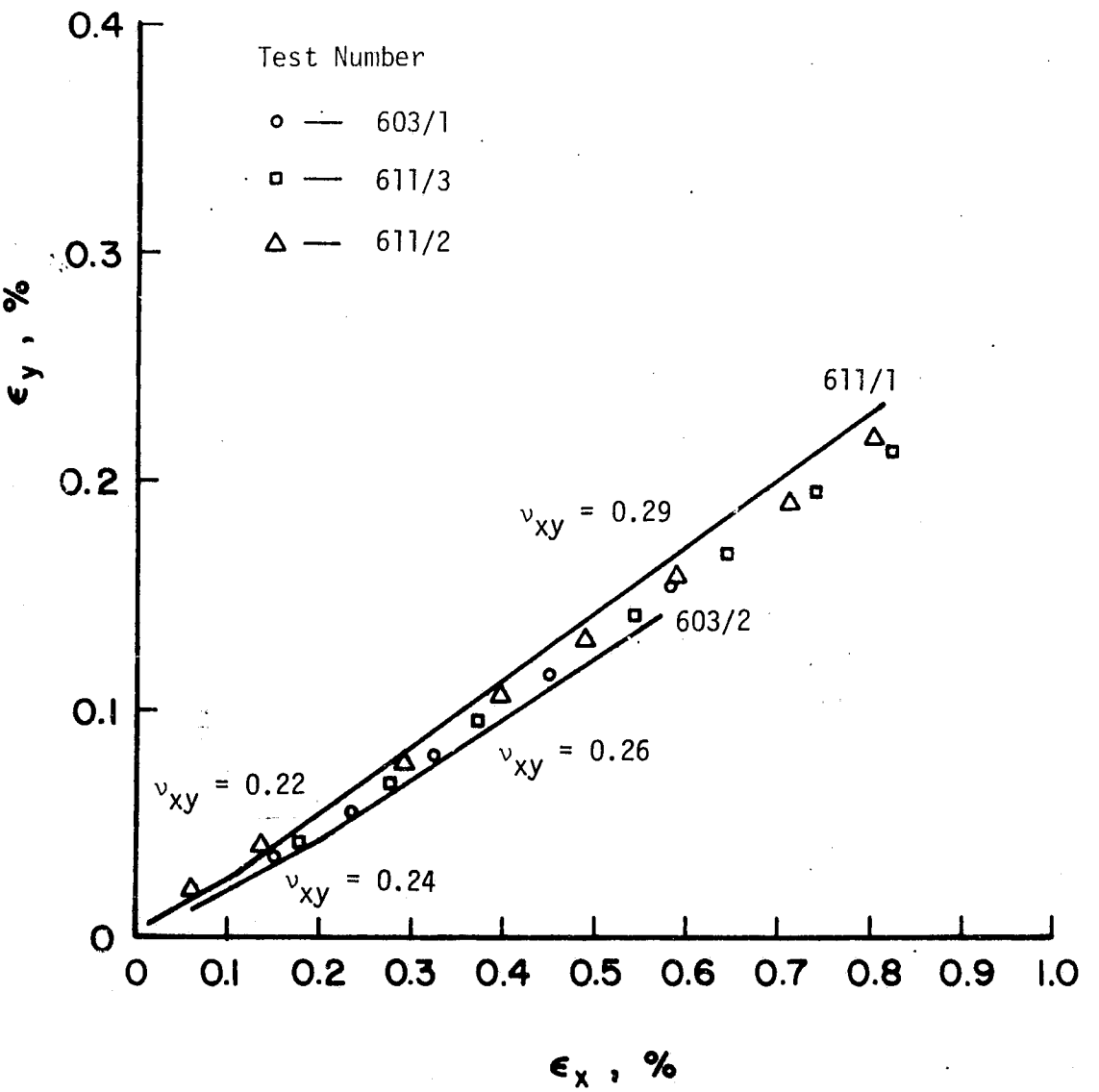

Figure 14. AXIAL STRAIN VS. TRANSVERSE STRAIN FOR $[0_8]$ TENSION TESTS

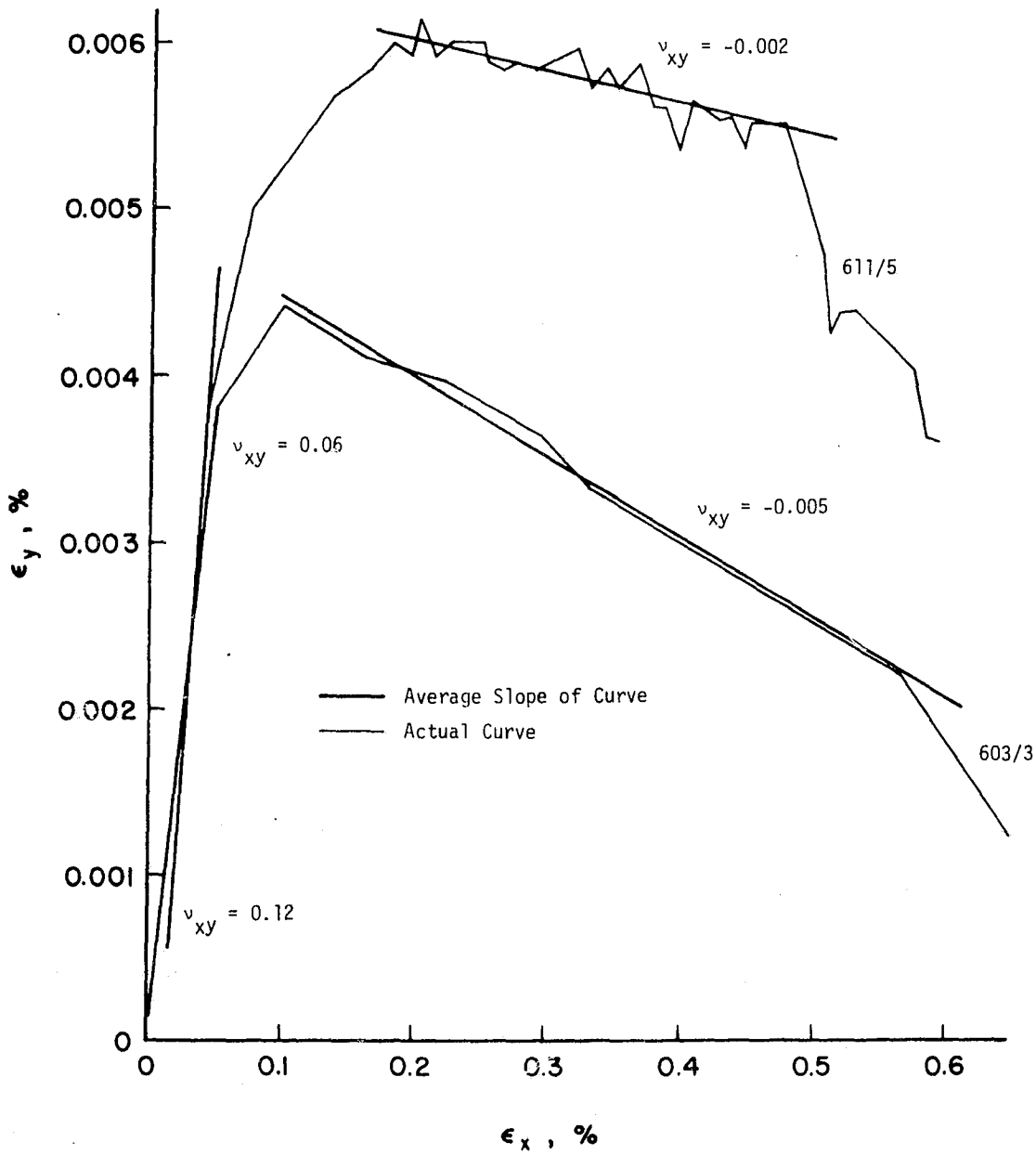

Figure 15. AXIAL STRAIN VS. TRANSVERSE STRAIN FOR $[90_8]$ TENSION TESTS

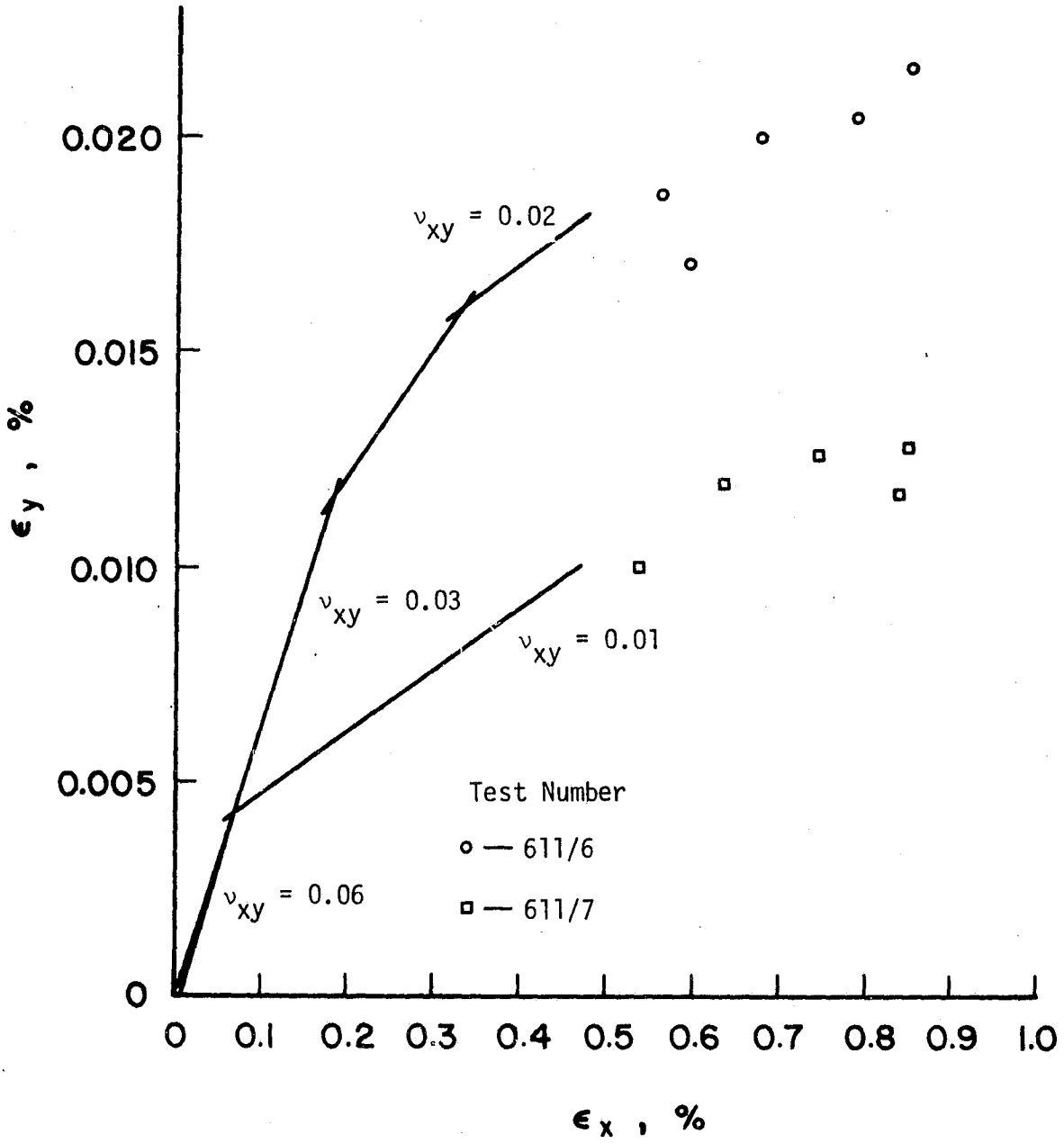

Figure 16. AXIAL STRAIN VS. TRANSVERSE STRAIN FOR $[(0/90_2]_s$ TENSION TESTS

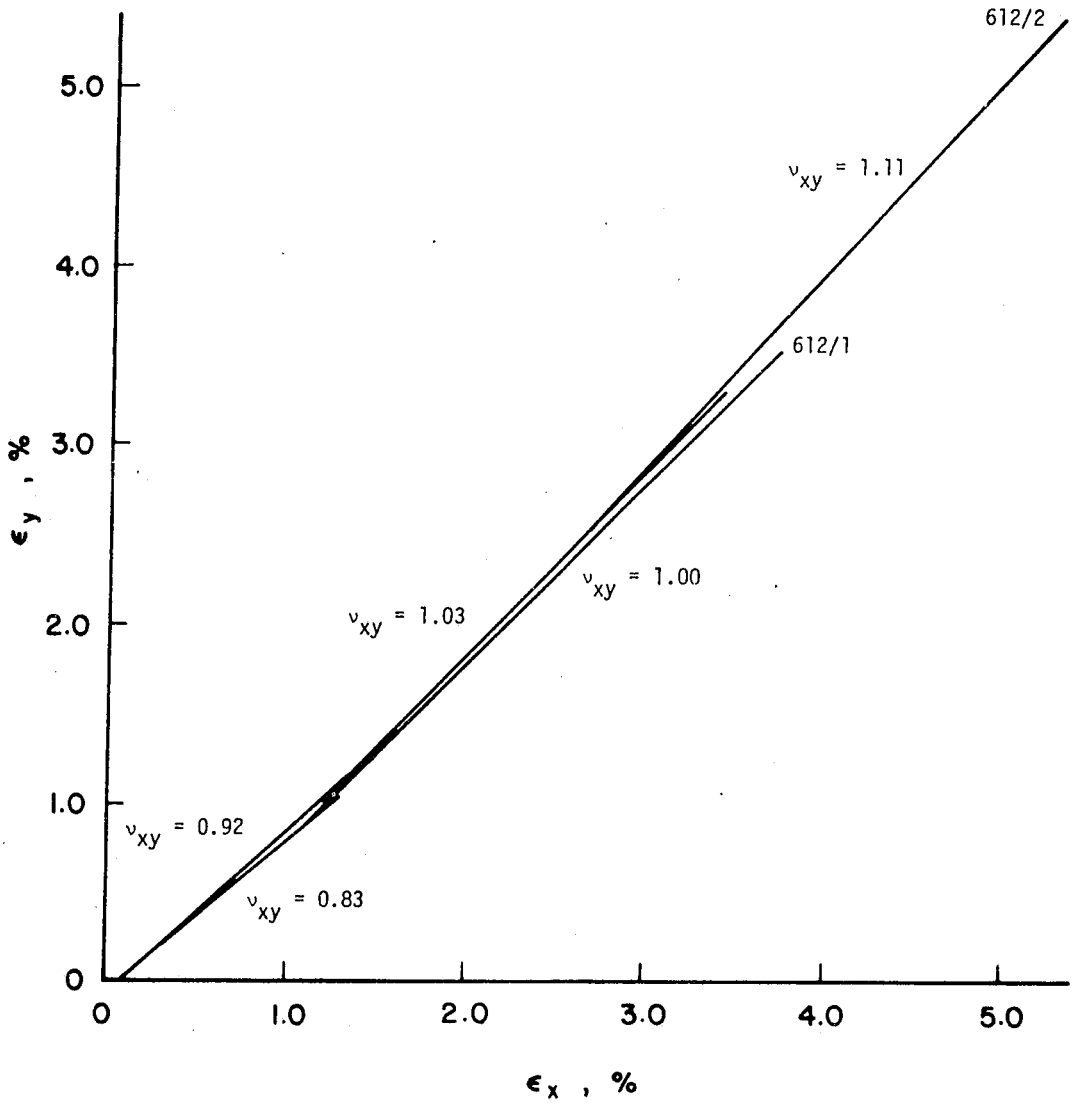

Figure 17. AXIAL STRAIN VS. TRANSVERSE STRAIN FOR $[+45/(-45)_2/(+55)_2/(-45)_2/+55]$ TENSION TESTS

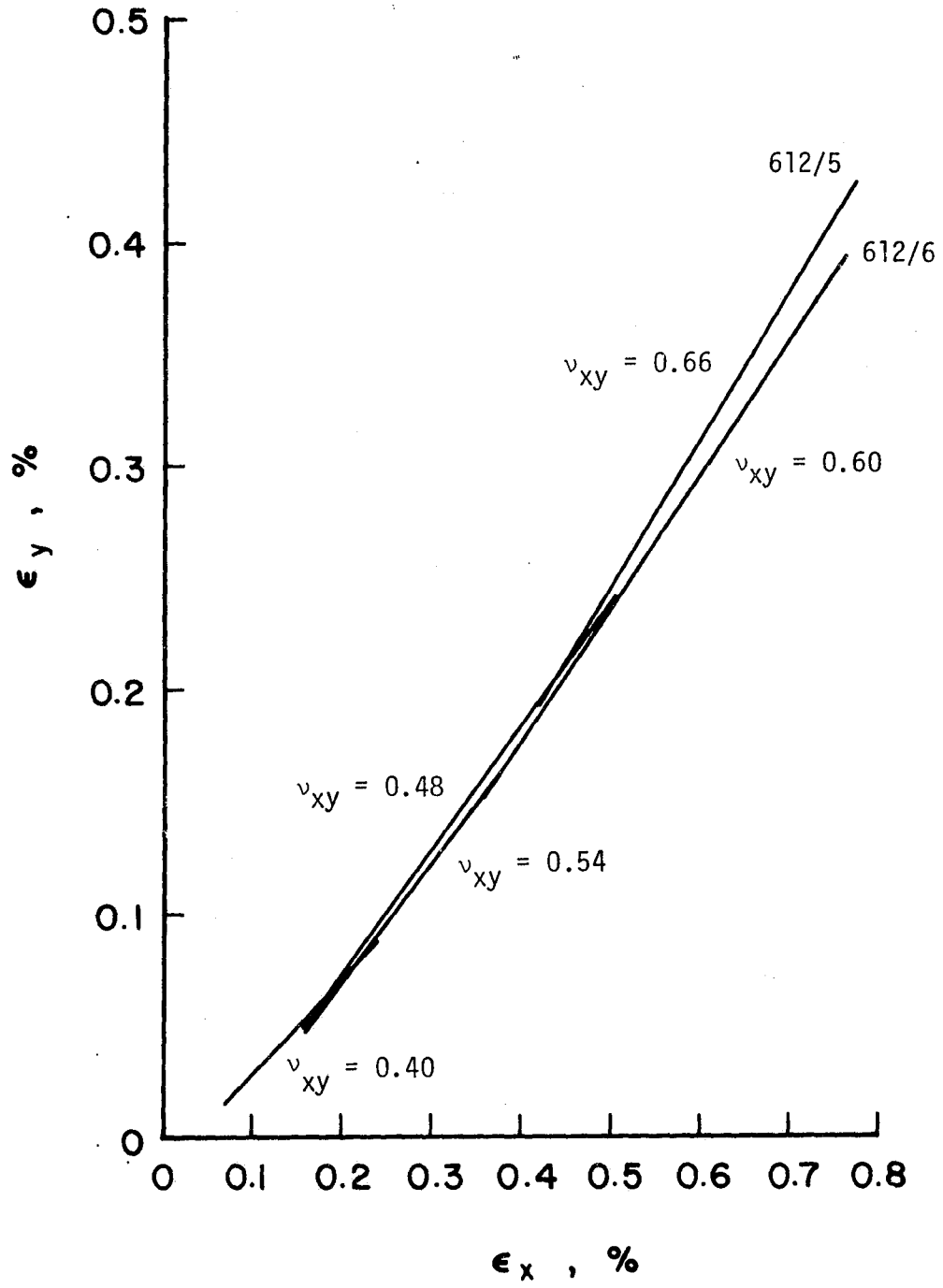

Figure 18. AXIAL STRAIN VS. TRANSVERSE STRAIN FOR $[0/\pm45]_s$ TENSION TESTS

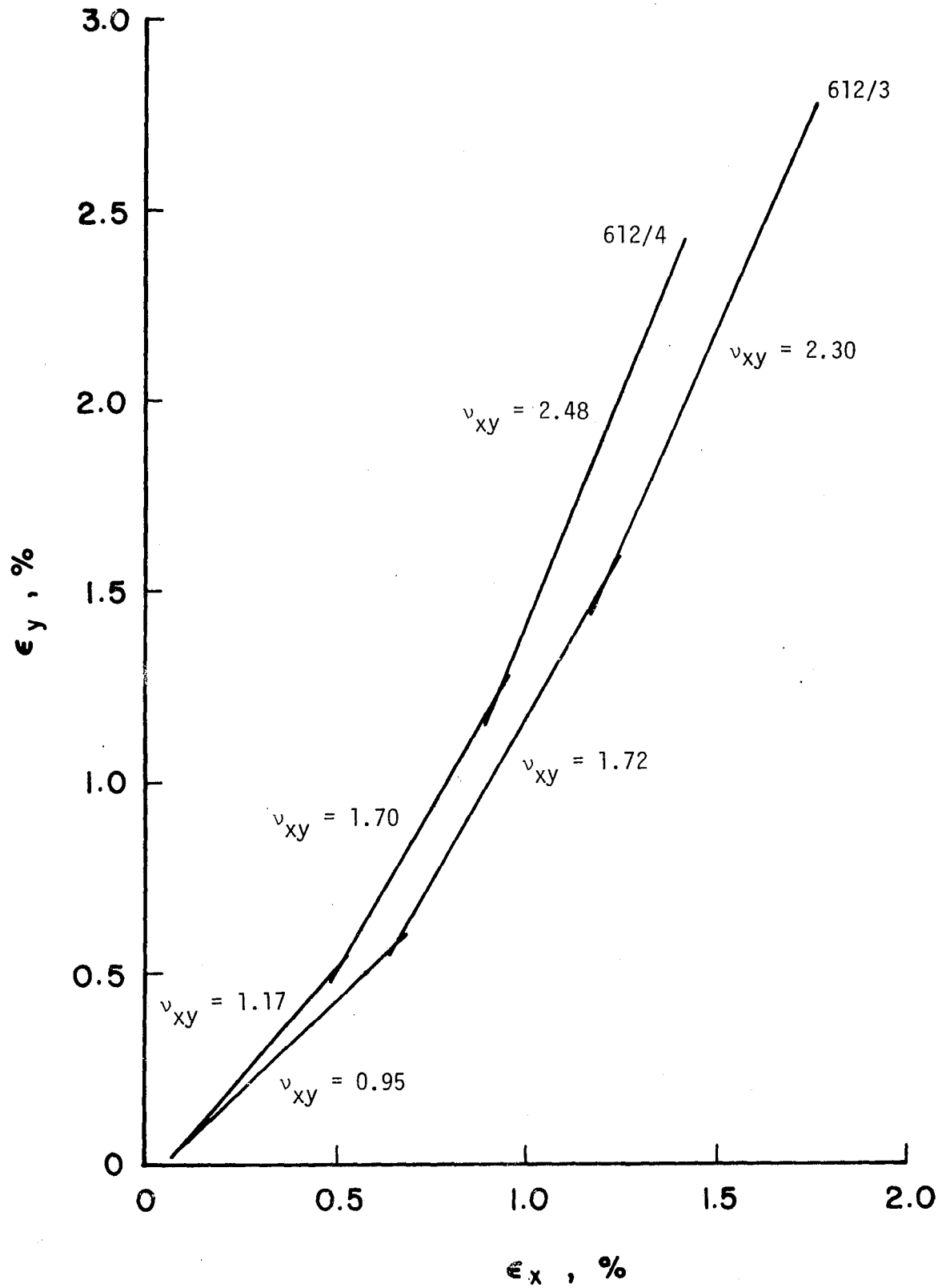

Figure 19. AXIAL STRAIN VS. TRANSVERSE STRAIN FOR $[(\pm 30)_2]_s$ TENSION TESTS

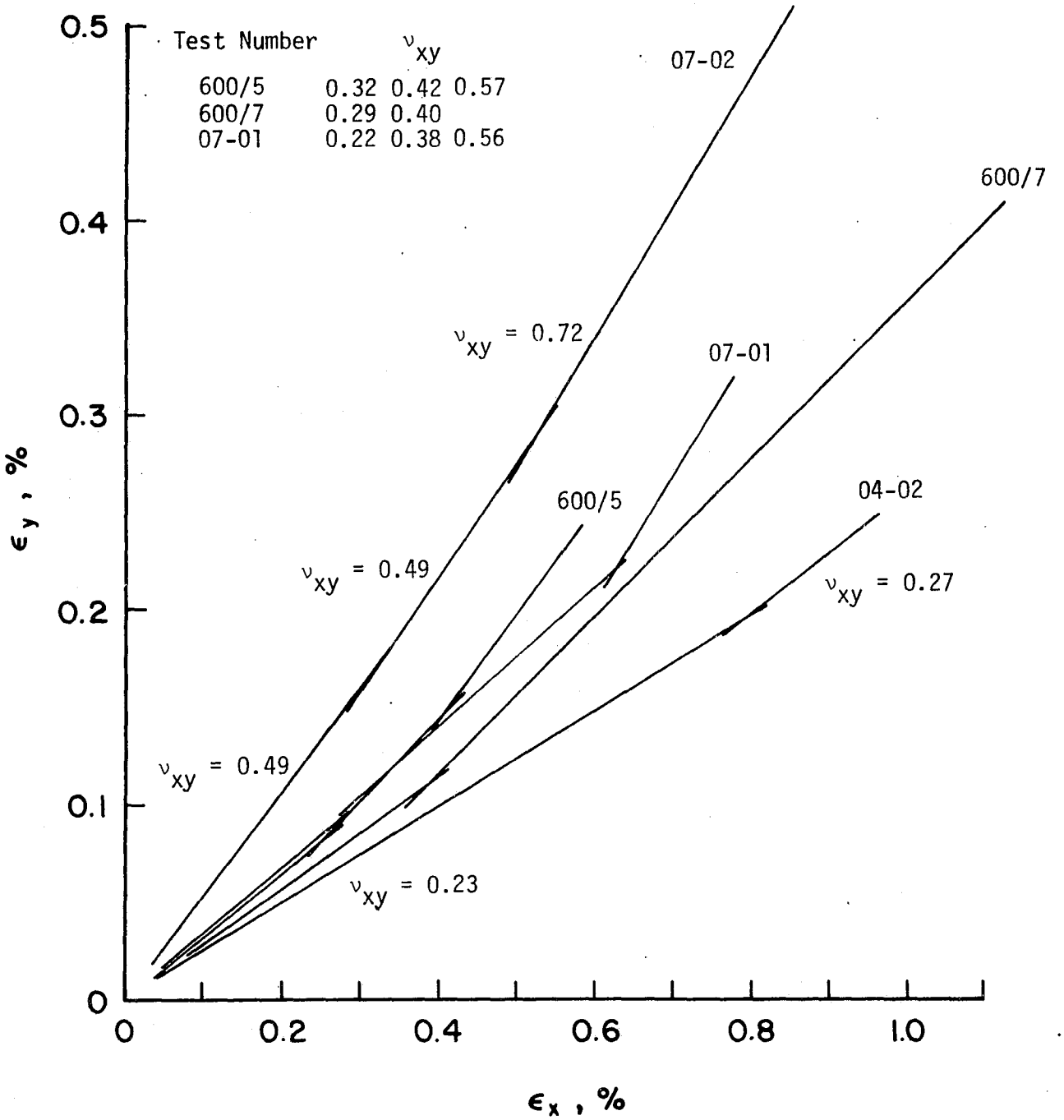

Figure 20. AXIAL STRAIN VS. TRANSVERSE STRAIN FOR $[0_4]$ COMPRESSION TESTS

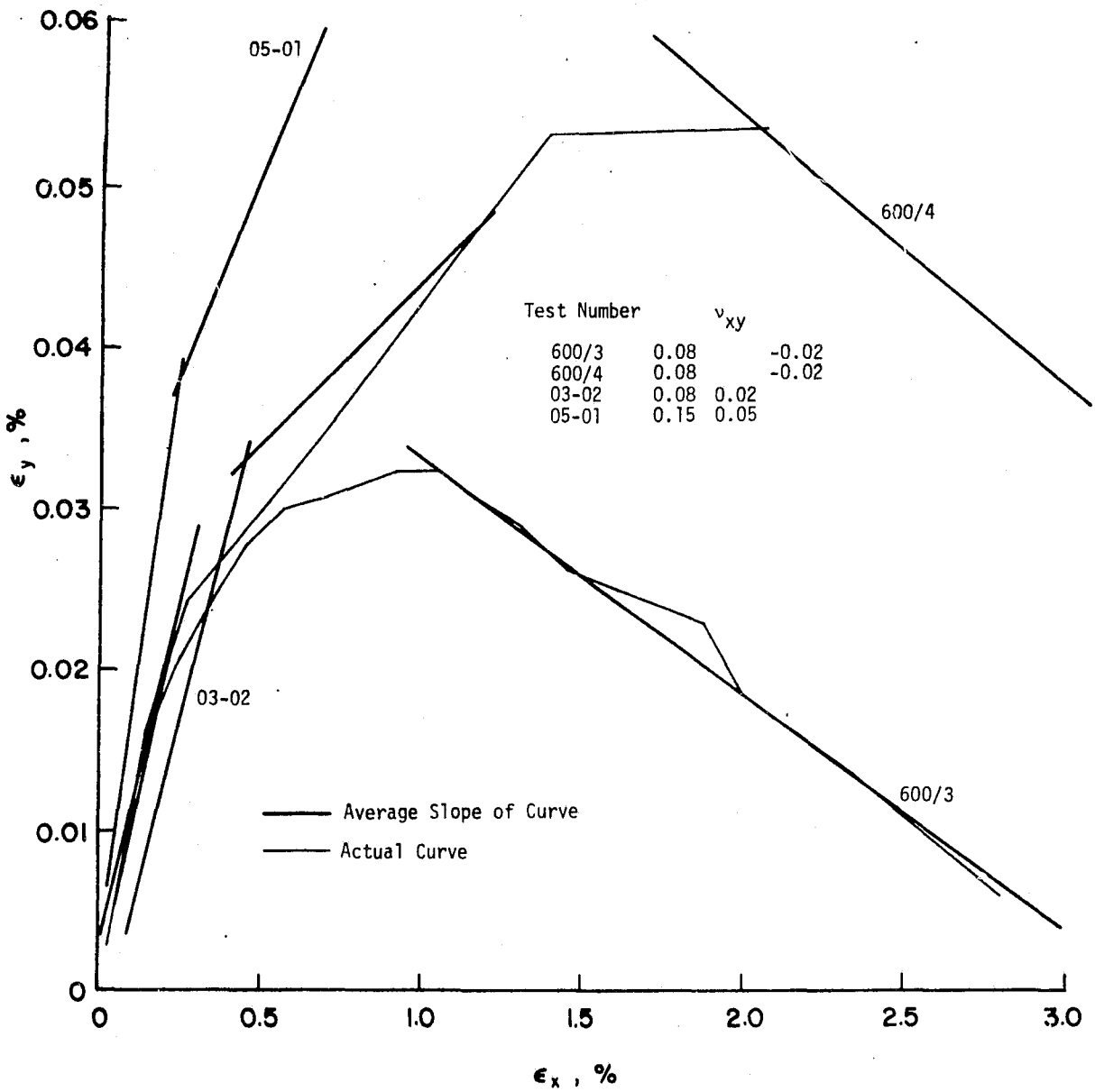

Figure 21. AXIAL STRAIN VS. TRANSVERSE STRAIN FOR $[90_8]$ COMPRESSION TESTS

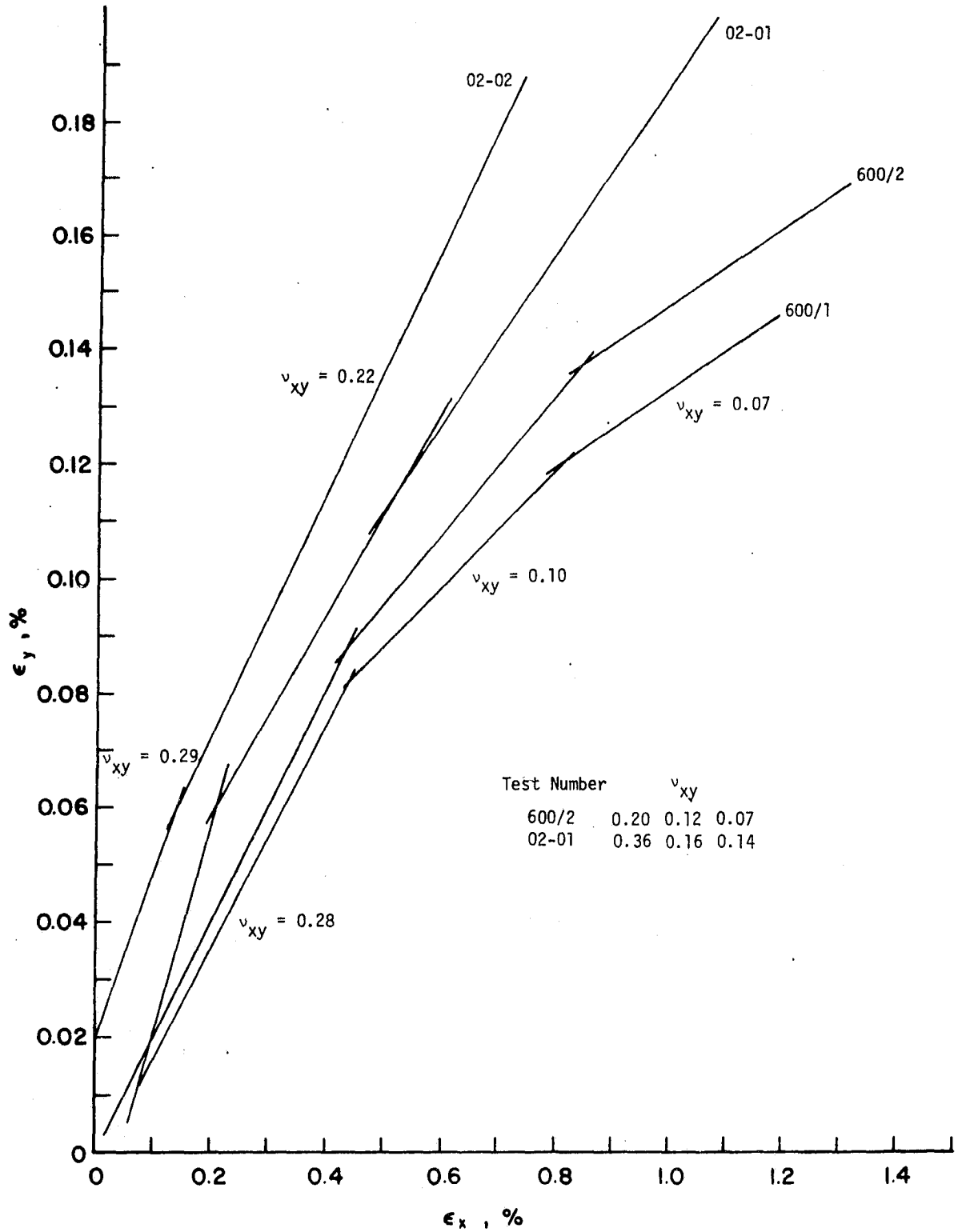

Figure 22. AXIAL STRAIN VS. TRANSVERSE STRAIN FOR $[(0/90)_2]_s$ COMPRESSION TESTS

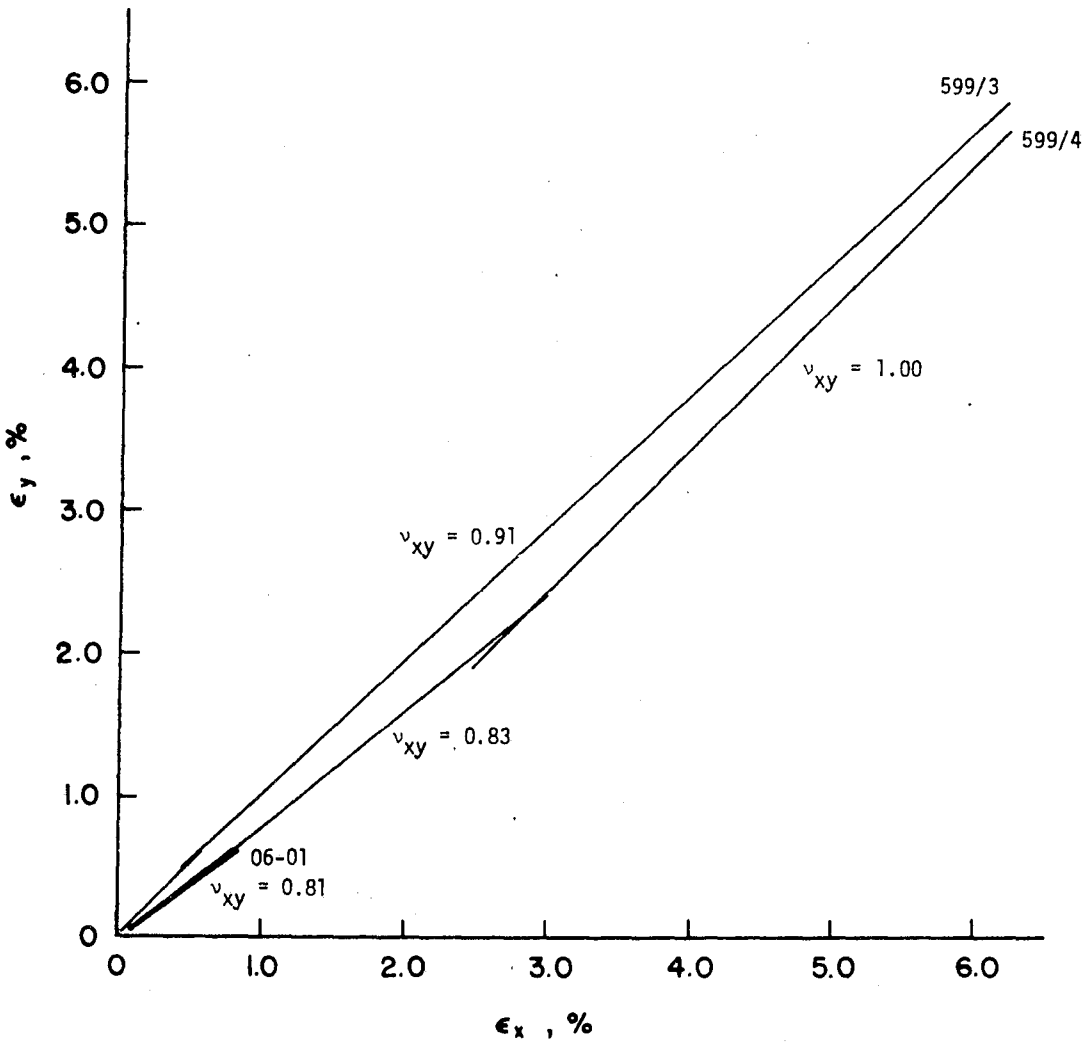

Figure 23. AXIAL STRAIN VS. TRANSVERSE STRAIN FOR $[+45/(-45)_2/+45]_s$ COMPRESSION TESTS

Note: 599/4 is a tension test

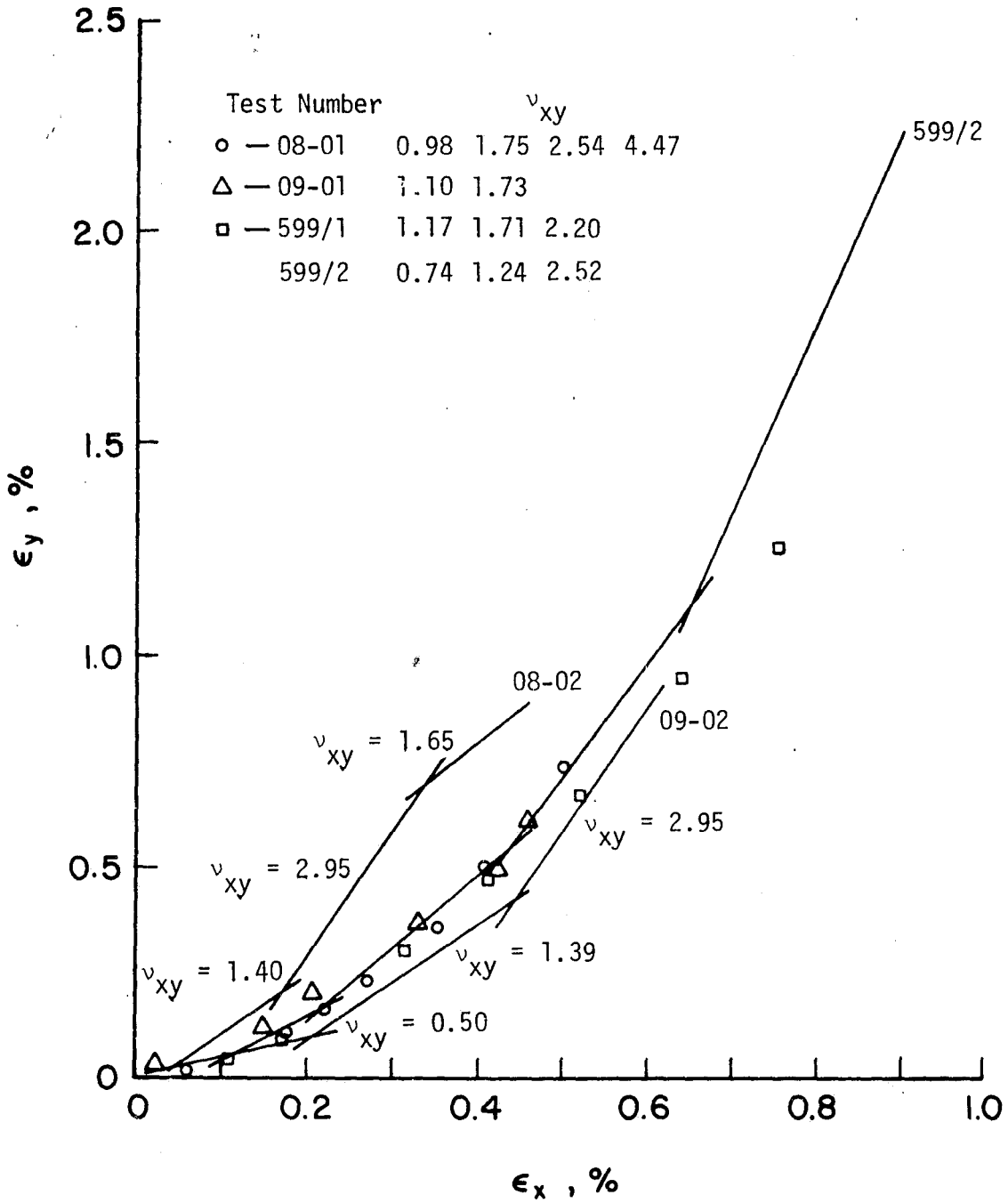

Figure 24. AXIAL STRAIN VS. TRANSVERSE STRAIN FOR $[(\pm 30)_2]_s$ COMPRESSION TESTS

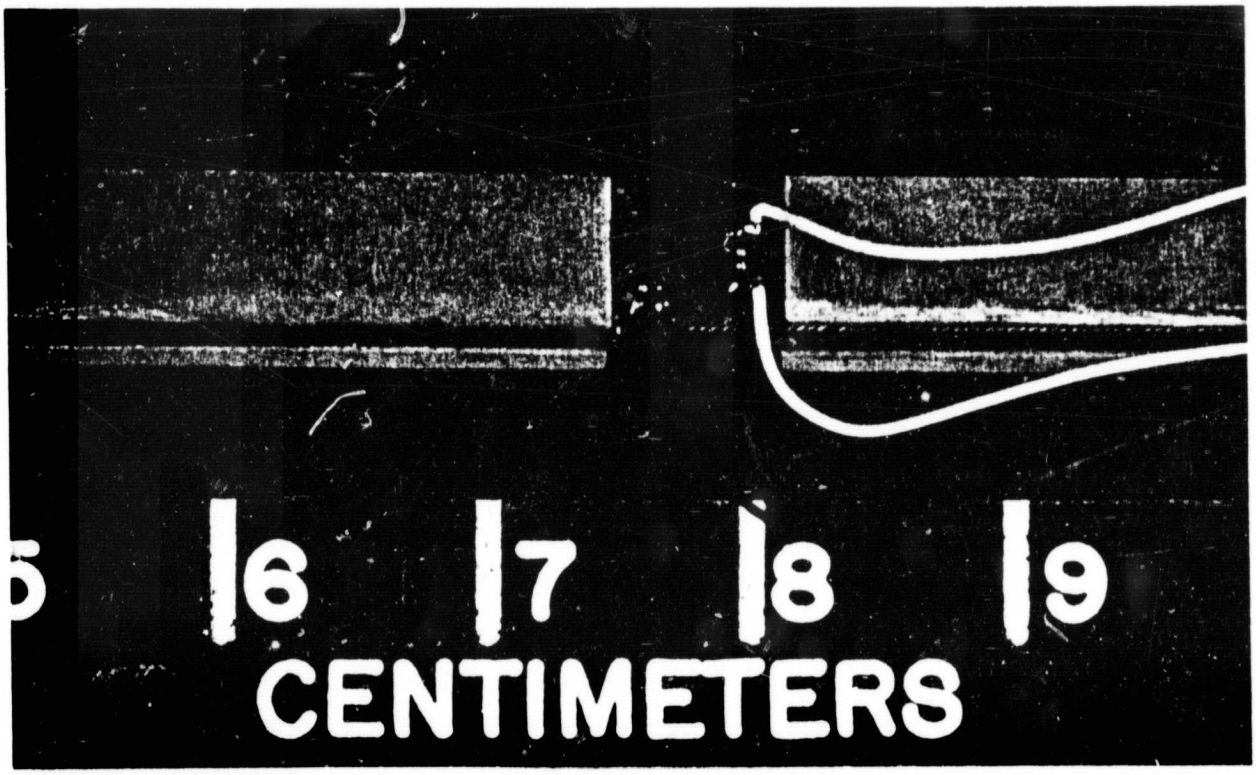

Figure 25. STRAIN GAGE LOCATIONS ON TYPICAL IITRI TEST SPECIMEN